
ORIGINAL ARTICLE**Journal Section**

A Process Model of Causal Reasoning

Zachary J. Davis¹ | Bob Rehder¹

¹Department of Psychology, New York University, 6 Washington Place, New York, NY 10003 USA

Correspondence
Zachary J. Davis, Department of Psychology, New York University
Email: zach.davis@nyu.edu

Funding information

How do we make causal judgments? Many studies have demonstrated that people are capable causal reasoners, achieving success on tasks from reasoning to categorization to interventions. However, less is known about the mental processes used to achieve such sophisticated judgments. We propose a new process model—the *mutation sampler*—that models causal judgments as based on a *sample* of possible states of the causal system generated using the Metropolis-Hastings sampling algorithm. Across a diverse array of tasks and conditions encompassing over 1,700 participants, we found that our model provided a consistently closer fit to participant judgments than standard causal graphical models. In particular, we found that the biases introduced by mutation sampling accounted for people's consistent, predictable errors that the normative model by definition could not. Moreover, using a novel experimental methodology, we found that those biases appeared in the samples that participants explicitly judged to be representative of a causal system. We conclude by advocating sampling methods as plausible process level accounts of the computations specified by the causal graphical model framework and highlight opportunities for future research to identify not just *what* reasoners compute when drawing causal inferences, but also *how* they compute it.

KEY WORDS

sampling, causal representation, causal reasoning, process models

1 | INTRODUCTION

The representation and use of causal knowledge is a central object of investigation in the cognitive sciences. Causal knowledge has been found to affect cognition in a wide variety of inference problems, from reasoning and learning to decision-making and categorization (for summaries, see Rottman & Hastie, 2014; Waldmann & Hagmayer, 2013). One formal model of the representation of causal knowledge—causal graphical models—has achieved success in modeling human performance across these tasks. A well-known advantage of causal graphical models is that they provide a compact representation of a causal system—only the local relations between a variable and its causal parents need be explicitly represented. Another is that they are accompanied by formal methods that specify how a causal model should be learned from observed data, used to draw inferences (including counterfactual judgments and the effects of interventions by an external agent), and updated in light of changing conditions (e.g. a malfunctioning component). However, causal graphical models are understood to provide a *computational level* account of causal cognition. Like all such accounts they specify *what* but not necessarily *how* specific computations are carried out (Anderson, 1990; Marr, 1982). This article extends this past work by proposing a new *rational process model* of the cognitive mechanisms that underlie many causal judgments. As a process model, the goals of this account include explaining why people commit the causal reasoning errors they do and how the correct inferences they draw can be computed within the resource limitations imposed by the human cognitive system.

1.1 | Sampling

Bayesian modeling has provided an influential account of human cognition (Griffiths et al., 2010). However, because these models are often highly computationally expensive, they are generally regarded as computational level accounts of behavior. Recently, a major project has been under way in the cognitive sciences to identify the processes by which people are able to approximate the normative Bayesian standard. Generally, researchers look for models that are minimally resource intensive but will still, at asymptote, converge to the correct answer. Monte Carlo methods are a natural approach to this resource-accuracy tradeoff. In particular, this paper deals with a popular variant of Monte Carlo methods—Markov chain Monte Carlo (MCMC)—that has achieved particular success in modeling cognition. For more extensive treatment of Monte Carlo methods and their uses in cognitive science, see Dasgupta et al. (2017).

MCMC models have successfully accounted for systematic biases across a variety of tasks. In one of the first applications of sampling methods to cognition, Lieder et al. (2012) showed that a simple MCMC model replicates the classic anchoring and adjustment effect (Tversky and Kahneman, 1974). It has been argued that taking a limited number of samples can be rational when taking into account things such as time costs (Vul et al., 2014) or the utility of exaggerated differences between decisions (Hertwig and Pleskac, 2010). Dasgupta et al. (2017) proposed MCMC models as a unified account of how people approximate Bayes' rule, capturing diverse phenomena such as the crowd within (Vul and Pashler, 2008) or self-generation (Koehler, 1994) effects. Sampling accounts are not restricted to probability estimation tasks. For example, Johnson and Bussemeyer (2016) modeled deviations from expected utility theory as resulting from biased sampling from prospects.

1.2 | Sampling and Causal Models

We propose a model for resource-constrained inference using causal graphical models. In particular, we propose that, when reasoning about a causal system, people think about concrete cases—states of the causal system in which all relevant variables are instantiated with values. For example, consider the causal graph in Fig. 1A in which variables

Y_A and Y_B are causes of variable X . Because the variables in this network are assumed to be binary, the *state space* of this graph—the possible assignments to the three variables—consists of the eight states shown in Fig. 1B. Our model assumes that reasoners sequentially *sample* these states. Later we will show that these generated samples can be used to carry out the kinds of inferences that can be modeled with causal graphical models.

The current model fits in with the burgeoning field of resource-rational models of cognition, which explain failures to adhere to the normative model as resulting from resource limitations. As in other sampling accounts of cognition, our approach is a balancing act between two goals. On one hand, we aim to explain how people succeed at making sophisticated causal judgments. We do this by showing that a psychologically plausible number of samples can reproduce human-level causal inference. On the other hand, we also aim to model the consistent, predictable errors commonly observed in research on causal cognition, analogously to sampling accounts of the anchoring effect or prospect theory (Lieder et al., 2012; Johnson and Busemeyer, 2016). For example, people systematically violate the *Markov condition*, a foundational feature of causal graphical models that defines patterns of conditional independence among a graph's variables. This principle is crucial for statistical inference from causal graphical models (Pearl, 1988; Koller and Friedman, 2009), and has been argued to be necessary for a rigorous account of interventions (Hausman and Woodward, 1999). We describe the Markov condition and the empirical violations later.

The paper will proceed as follows. We first formalize our model, which we dub the *mutation sampler*. The mutation sampler embodies four principles, principles that we will show are sufficient to reproduce a variety of causal judgments. The first principle of course is sampling itself, that people think of concrete cases and ultimately draw inferences on the basis of those cases. The second is that each subsequent case that is sampled differs minimally from the previous one; in fact, it is formed by “mutating” the value of only a single graph variable. The third principle concerns the network state at which sampling commences. We present both psychological and computational arguments for why sampling should commence at certain network states that we will dub “prototype states.” The fourth principle is simply that of resource limitations, the inability of human reasoners to take a large number of samples. When combined with the other principles, small samples will be shown to account for the empirical phenomena we consider here.

Following the presentation of the mutation sampler, we compare fits of it and standard causal graphical models to empirical data from a wide variety of tasks and conditions. We first consider a canonical causal judgment, a conditional probability task in which a reasoner predicts the state of one variable given the state of other variables that are causally related. This section considers data from 19 experimental conditions over 8 distinct causal network topologies and focuses on the model's accounts of the systematic reasoner errors alluded to above (e.g., independence violations). We then ask if the mutation sampler's predictions generalize to other causal-based tasks, namely, judging category membership and choosing interventions to obtain a desired outcome. These two sections consider data from 28 experimental conditions involving 9 different causal structures. We then further consider whether the mutation sampler's predictions generalize to a completely novel causal-based task, one that is designed to test its assumption in relatively direct way. In the General Discussion we will compare the mutation sampler to other models of causal-based judgments.

To foreshadow, we show that the mutation sampler consistently provides a better fit to multiple types of causal judgments as compared to normative causal graphical models. This finding demonstrates that both the striking successes and systematic errors that people make when reasoning about causal systems can be accounted for by the assumption that they reason on the basis of a modest number of samples taken from the possible states of a causal system rather than computing a normative response. We will conclude by advocating the framework of sampling methods as plausible process level accounts of the computations specified by the causal graphical model framework.

2 | THE MUTATION SAMPLER

As mentioned above, the proposed model is a sampling algorithm that implements a few key principles of causal inference. The sampling algorithm we choose—Metropolis-Hastings (MH) Markov Chain Monte Carlo—is a rational process model in that it asymptotically converges to the optimal response. Of course, there are many possible sampling algorithms that also converge, and future work could discriminate between these algorithms through a resource rational analysis (Griffiths et al., 2015). Instead, the mutation sampler uses MH as an implementation of its key principles. See the General Discussion for another sampling algorithm—the Gibbs sampler—that also fits people’s behavior well, but only if all four key principles hold.

2.1 | Principle 1: Sampling Concrete Cases

The proposed model is a variant of Metropolis-Hastings (MH) Markov Chain Monte Carlo, a computationally efficient rejection sampling method for estimating probability distributions (Hastings, 1970; Van Ravenzwaaij et al., 2018). MH methods sample from a distribution in a manner that ensures that the generated samples will, after normalization, approximate the original distribution, with convergence guaranteed as the size of the sample grows large. Whereas MH models often deal with a continuous state space, the proposed model samples over the discrete states of a causal graph – like the one in Fig. 1. Just as with any distribution, the joint probability distribution associated with this graph can be approximated via MH sampling over its states. Note that our psychological claim will be that people make causal judgments on the basis of the samples they draw from a causal graph without necessarily forming a normalized joint distribution. The unnormalized joint distribution represented by the sample is sufficient to model the inferences that can be computed from a causal graphical model.

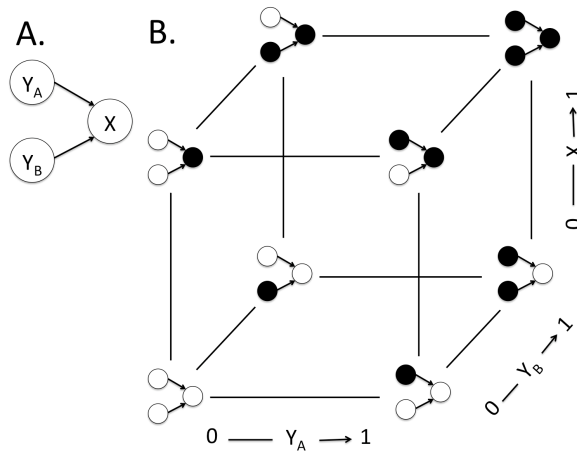


FIGURE 1 (A) A common effect graph. (B) Possible states of a common effect graph. Filled circles indicate a variable instantiated with a value of 1, open circles one with a value of 0. Edges denote reachable states as defined by the mutation sampler’s proposal distribution.

Like all MCMC methods, MH constructs a sequence (or chain) of samples, where the choice of each subsequent sample in the chain depends on the previous sample. Specifically, MH is defined by two components: a proposal

distribution $\mathbb{Q}(q'|q)$ and a transition probability $a(q'|q)$ where q is the current state and q' is the proposal state in a random walk. The standard MH transition probability $a(q'|q)$ determines whether the next state in the chain should repeat the current state q or involve a transition to the new state q' and is defined by,

$$a(q'|q) = \min\left(1, \frac{\pi(q')}{\pi(q)}\right)$$

where $\pi(q)$ is the joint probability of the causal system being in state q . Importantly, $a(q'|q)$ only requires the computation of the *relative* probability of two system states, $\pi(q')$ and $\pi(q)$. This property is key because it means that $a(q'|q)$ can be computed without access to the graph's full joint distribution, which of course is what the sampling process is attempting to approximate.

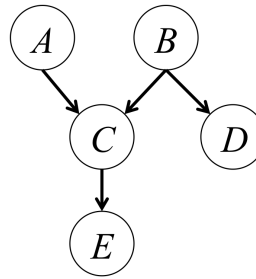
2.2 | Principle 2: Mutation Proposal Distribution

The proposal distribution $\mathbb{Q}(q'|q)$ determines which graph state should be proposed as the next state in the chain (i.e., the state that will play the role of q' in the computation of $a(q'|q)$). We assume a $\mathbb{Q}(q'|q)$ that restricts reachable states q' to those that differ from the current state q by the value of one binary variable. The mutation sampler derives its name from the fact that potential proposals are those formed by “mutating” the value of a single variable. Each mutated (reachable) state has an equal probability of being selected as a proposal. Edges in Fig. 1B denote reachable states from some starting state. This proposal distribution was inspired by models in other domains that assume the proposal distribution makes small adjustments to the currently held state (Bramley et al., 2017; Johnson and Busemeyer, 2016; Lieder et al., 2012). In addition, later we present experimental results that provide direct empirical support for this proposal distribution.

Note that this proposal distribution confers additional efficiency benefits. Because only one variable V_i is changed, the ratio $\frac{\pi(q')}{\pi(q)}$ simplifies to

$$\frac{\pi(v'_i, v_{-i})}{\pi(v_i, v_{-i})} = \frac{\pi(v'_i|v_{-i})\pi(v_{-i})}{\pi(v_i|v_{-i})\pi(v_{-i})} = \frac{\pi(v'_i|v_{-i})}{\pi(v_i|v_{-i})} = \frac{\pi(v'_i|u_i)}{\pi(v_i|u_i)}$$

where v_i and v'_i are the values of variable V_i in q and q' , respectively, and u_i denotes the state of the variables in V_i 's *Markov blanket*. By definition, variables outside V_i 's Markov blanket are independent of V_i given u_i ; thus, $\pi(v_i|v_{-i}) = \pi(v'_i|u_i)$ is entailed. In a causal graphical model, a variable's Markov blanket includes its direct parents, its direct children, and the other direct parents of its direct children (Koller and Friedman, 2009). It is often convenient to again express $\frac{\pi(q')}{\pi(q)}$ as the relative likelihood of two (now partial) network states by noting that $\frac{\pi(v'_i|u_i)}{\pi(v_i|u_i)} = \frac{\pi(v'_i,u_i)\pi(u_i)}{\pi(v_i,u_i)\pi(u_i)} = \frac{\pi(v'_i,u_i)}{\pi(v_i,u_i)}$. Examples of variables' Markov blanket and the resulting simplification of $\frac{\pi(q')}{\pi(q)}$ are presented in Fig. 2; quantitative examples of the calculation of MH transition probabilities are presented in Appendix A. In particular, Appendix A demonstrates how those transition probabilities reduce to simple expressions involving only the local probabilities that define how variables are generated from their parents (known as a graph's *conditional probability distributions*, or CPDs). The fact that CPDs are assumed to be explicitly represented as part of a causal graphical model means that a chain of samples can be generated with exceptional efficiency. The General Discussion will consider additional efficiencies that can be realized depending on the particular causal judgment a reasoner is faced with.



Mutated variable	Markov blanket	Metropolis-Hastings ratio
E	C	$\pi(ce')/\pi(ce)$
A	B, C	$\pi(a'bc)/\pi(abc)$
C	A, B, E	$\pi(abc'e)/\pi(abce)$

FIGURE 2 Examples of the calculation of Metropolis-Hastings ratio. When the mutated variable is E , $\pi(q')/\pi(q)$ reduces to $\pi(ce')/\pi(ce)$ because E 's Markov blanket consists of only C . That is, for purposes of this calculation the states of A , B , and D in q and q' can be ignored. When the mutated variable is A , the calculation of $\pi(q')/\pi(q)$ can ignore the state of D and E . When the mutated variable is C , it can ignore the state of D .

2.3 | Principle 3: Biased Starting Points

The model thus far is simply an efficient MH sampler for estimating a causal graph's joint distribution. Importantly, however, we introduce a bias in the starting point for sampling: Sampling always starts from one of the 'prototype' states, those in which nodes are either all present (0) or all absent (1). For example, for the network in Fig. 1A, the prototypes are the bottom left and top right corners of Fig. 1B, states referred to as $y_A^0y_B^0x^0$ and $y_A^1y_B^1x^1$, respectively.¹

We suggest that prototypes readily come to mind as plausible states at which to start sampling because they are guaranteed to be consistent with the causal relations. Because the prototypes include no instances in which a cause is present but an effect absent (or vice versa), the reasoners can identify them as consistent with the causal relations without attending to aspects of the causal graph such as the strength, direction, or functional form of the causal relations. In fact, Appendix B demonstrates that this assumption is not only psychologically plausible, it often leads to more accurate causal inferences for a given sample size. This finding reflects the fact that the prototypes often are the high probability states of a causal system with generative causal links, so starting with these states results in quicker convergence to the true joint distribution. Note that the General Discussion will consider generalizations of the mutation sampler to causal graphs with inhibitory causal links. There we will consider the appropriate points to start sampling from such graphs.

We also propose that, depending on the domain being reasoned about, one of the two prototype states may come to mind more readily than the other. For example, some of the empirical studies we analyze later taught participants novel categories with inter-feature causal relations and explicitly informed them that some category features are more likely than others. In such cases, we introduce a *bias* parameter that adjusts the probability of initializing the chain at each prototype. Unless otherwise mentioned, *bias* is set to .50, meaning that the chain is equally likely to be initialized at either prototype state.

¹Throughout this article we use lowercase and superscripts to denote the state of a variable, that is, $v_i^j \equiv V_i = j$. Thus, x^0 denotes that X is absent, y_A^1 that Y_A is present, and so forth.

2.4 | Principle 4: Limited Capacity

Regardless of our proposal distribution and biased initialization, the chain of samples generated by the mutation sampler is guaranteed to converge to the normative joint distribution as defined by the causal graphical model. However, convergence is likely only when the number of samples is large. In contrast, we assume that people are resource-constrained and thus can only take a few samples (on the order of a dozen rather than thousands or millions). Following Bramley et al. (2017), we assume that people have a fixed *capacity* for sampling but vary in the number of samples taken for any particular judgment, albeit with the constraint that at least two samples are drawn (the initial prototype and one more). To instantiate these constraints, for each judgment we draw from a Poisson distribution with mean λ' a quantity k' ; the number of samples taken is $k = k' + 2$ (and so the mean number of samples is $\lambda = \lambda' + 2$). Larger λ values signify that a participant has a capacity to take many samples and so would behave more in line with a normative causal graphical model. Smaller λ values signify a limited capacity to take samples and thus a stronger divergence from the normative model. In particular, when λ is small the mutation sampler will not have time to fully explore the state space and so will overestimate the probability of states near the starting point and underestimate the remaining states.

These effects are illustrated in Fig. 3, which presents the joint distributions derived by the mutation sampler for two types of graphs: a common effect graph (panel A) and a common cause graph in which X is a cause of Y_A and Y_B (panel B). The blue lines with closed plot points represent the normative joint distribution—that is, for each of the eight possible graph states, the (joint) probability of that state—generated by the causal graphical model under a particular parameterization (computed via the standard methods defined in Appendix A).² The red lines with open plot points represent approximations of that distribution derived from the mutation sampler for three different values of λ : 4, 8, and 32. To make the predictions of the mutation sampler comparable to the normative model (and each other), the samples it generates have been normalized by dividing the number of visits to each state by the total number of samples.

A comparison of the joint distributions in Fig. 3 sheds insight into how the mutation sampler works. For both graphs, the joint probabilities for the prototype states estimated by the mutation sampler are greater than those derived from the normative model, a consequence of sampling beginning at those states. Conversely, the mutation sampler's joint probabilities for the remaining network states are less than those of the normative model. We argue that the fact that mutation sampling reproduces the general shape of the true joint distribution explains why people draw approximately veridical causal inferences. The systematic deviations from that joint explains the common errors they make. Note that the magnitude of those deviations vary with the average sample size λ . By the time that λ equals 32, the discrepancy between the joint distributions of the mutation sampler and the normative model has become very small, confirming that the mutation sampler converges to the normative model when the resources required for extensive sampling are available.

Also note that the mutation sampler's predictions in Fig. 3 represent the joint distributions' expected values rather than a single run of the sampler. These expected values can be computed analytically. First, the distribution over the graph states representing which are likely to be the current state at sample n can be computed by multiplying the distribution at sample $n - 1$ by the matrix of transition probabilities between graph states defined by the Metropolis-Hastings rule (the initial distribution before sampling commences is .50 at the two prototypes and 0 otherwise). Sum-

²The probabilities in Fig. 3 match what states intuition indicates should be more or less likely in light of the causal relations. For both causal graphs the prototype states in which variables are either all absent ($y_A^0 y_B^0 x^0$) or all present ($y_A^1 y_B^1 x^1$), shown on the far left and right, respectively, of each panel, are highly probable states. For the common effect graph, states in which the effect X is accompanied by one cause ($y_A^1 y_B^0 x^1$ and $y_A^0 y_B^1 x^1$) are moderately probable whereas the state where both causes are present but the effect absent ($y_A^1 y_B^1 x^0$) is quite improbable. For the common cause graph, states in which the cause X is accompanied by one effect ($x^1 y_A^0 y_B^1$) and ($x^1 y_A^1 y_B^0$) are moderately probable whereas one where both effects are absent ($x^1 y_A^0 y_B^0$) is not.

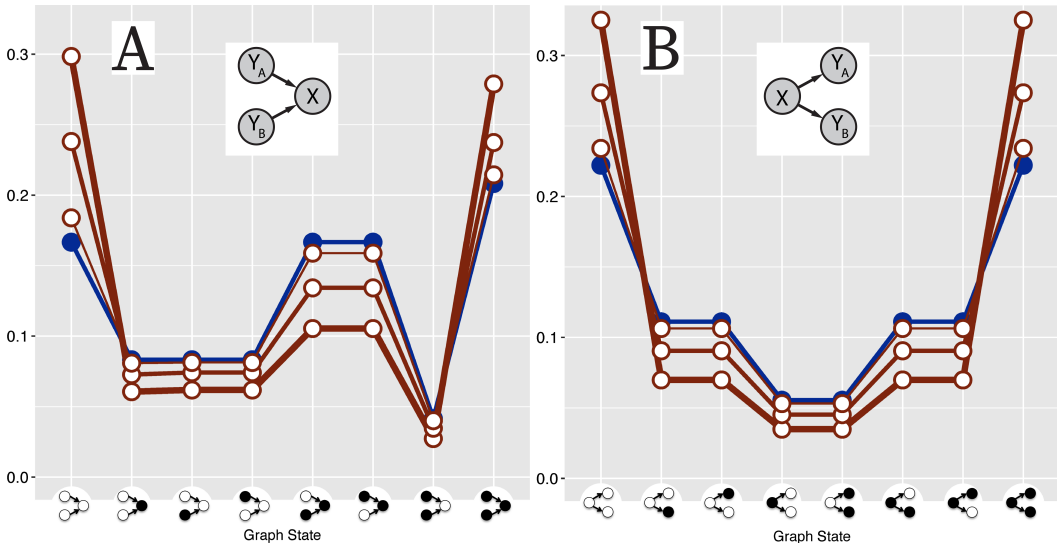


FIGURE 3 Joint probability distributions for (A) a common effect graph and (B) a common cause graph. The horizontal axis presents graph states in the same format as Fig. 1 (i.e., filled circles indicate a 1, open circles a 0). Causal relations in both networks are assumed to be generative, independent, and combine according to a noisy-or integration function (see Appendix A). Both networks are parameterized such that the marginal probability of the causes = .50, the causal strength = .50, and the strengths of background causes = .33. The blue line (closed plot points) represents the joint distribution entailed by the normative model. Red lines (open plot points) represent the joint distributions implied by the mutation sampler, with thicker lines meaning fewer samples (thick: $\lambda = 4$; medium: $\lambda = 8$; thin: $\lambda = 32$).

ming these distributions yields the expected number of visits to each graph state after n samples. Then, the expected joint associated with a given λ can be computed by taking a weighted average of the distributions computed at every chain length.³ Nevertheless, remember that our psychological claim is that reasoners run a single chain of samples for each causal judgment. We will consider some consequences of that claim (e.g., the inherent variability of causal judgments) in the General Discussion.

2.5 | Example Run

The previous sections formalized how the mutation sampler generates a sequence of samples. However, it may be helpful to see an example of the process at work. Table 1 shows a single run of the mutation sampler for the common effect graph in Fig. 1A. The chain starts at one of the prototype states, in this case $y_A^1 y_B^1 x^1$. Then, a proposal that differs by only one variable ($y_A^1 y_B^0 x^1$) is generated. The MH ratio (the ratio of the proposal state's probability to the current state's probability) is calculated and compared to a random number generated from $Unif(0, 1)$ (refer again to Appendix A for the calculation of MH ratios). If the ratio is greater than the random number, the current state is

³Because in a Poisson distribution the probability of any value of k' is non-zero, we clipped that distribution so as to consider the values of k' that accounted for .999 of the distribution. For example, the values of k' from 0 to 15 account for .999 of a Poisson distribution with a mean of 8. We thus computed the 16 joint distributions associated with the values of k' of 0, 1, ..., 15 and then averaged those joints, each weighted by their probability (as specified by the Poisson distribution).

state (q)	proposal (q')	$\frac{\pi(q')}{\pi(q)}$	$Unif(0, 1)$	ratio > rand?
$y_A^1 y_B^1 x^1$	$y_A^1 y_B^0 x^1$.79	.32	True
$y_A^1 y_B^0 x^1$	$y_A^1 y_B^0 x^0$.54	.74	False
$y_A^1 y_B^0 x^1$	$y_A^1 y_B^1 x^1$	1.27	.84	True
$y_A^1 y_B^1 x^1$	$y_A^1 y_B^1 x^0$.21	.56	False
$y_A^1 y_B^1 x^1$	$y_A^1 y_B^0 x^1$.79	.38	True
$y_A^1 y_B^0 x^1$	$y_A^0 y_B^1 x^1$.46	.11	True
$y_A^1 y_B^0 x^1$	$y_A^0 y_B^0 x^0$	2.33	.29	True
$y_A^0 y_B^0 x^0$	$y_A^1 y_B^0 x^0$.50	.33	True
$y_A^1 y_B^0 x^0$	$y_A^0 y_B^0 x^0$	2.00	.80	True
$y_A^0 y_B^0 x^0$	$y_A^0 y_B^1 x^0$.50	.09	True
$y_A^0 y_B^1 x^0$

TABLE 1 Example run of the mutation sampler for a common effect graph (marginal probability of causes = .50, causal strength = .50, and strength of background causes = .33).

updated to the proposal state. If it is smaller, the proposal is rejected and the current state is unchanged. This process continues until a chain of the desired length is acquired.

As mentioned, the sequence of samples obtained by this process serves as an estimate of causal graph's joint distribution. The joint distribution estimated by a long chain of samples will be virtually indistinguishable from that specified by the normative model. The one estimated by a short chain will exhibit the sorts of deviations shown in Fig. 3. Once obtained, the estimated joint can then be used to carry out the inferences typically supported by causal graphical models.⁴ In particular, the fits of the mutation sampler to the multiple empirical studies that are presented in the following sections each first estimate a joint distribution and then compute the causal-based judgments that were presented in that study.

Although the strategy of generating a full joint distribution and then computing the needed inference is completely general, there are certain types of inferences for which even more efficient sampling strategies exist—in particular ones that sample only over those network states that are needed to compute the inference. In the General Discussion we will describe how the mutation sampler can incorporate such sampling strategies and the additional efficiencies obtained when it does so.

2.6 | Summary

We now summarize the key claims of the mutation sampler. First, the generally good performance of human causal reasoners is attributed to sampling network states in such a manner that the obtained sample approximates the causal network's true joint distribution (Principle 1). That sample can then be used to derive a variety of causal-based in-

⁴A technical question that arises is how to handle the instances of division by zero that may occur for certain types of inferences when the number of visits to relevant system states is zero. We generally avoid this issue because, as described above, the mutation sampler predictions we present are based on the *expected* number of visits to a system's states and the minimum number of samples taken is at least two, constraints that entail that the expected number of visits to each state will be greater than zero. However, exceptions occur for causal models with degenerate parameter values. For example, if the causal relation $C \rightarrow E$ in Fig. 2 is deterministically sufficient (C always produces E) then the expected number of visits to any state in which $C = 1$ and $E = 0$ will be 0 and the computations of, say, $p(a^1 | c^1 e^0)$ will involve division by zero. Similarly, if $C \rightarrow E$ is deterministically necessary (E has no causes other than C) then the expected number of visit to any state in which $C = 0$ and $E = 1$ will be 0. We handle such edge cases by initializing the number of visits to each state with a very small value (10^{-10}). The General Discussion will discuss mutation sampler predictions that are based on single chain of samples (rather than the expected number of visits to each state) and show how initializing the number of visits a small value may in fact have a role in explaining the variability associated with causal inferences.

Model	Principles Implemented	Causal Reasoning	Causal Categorization	Causal Interventions	Causal Representations
Normative		5506.6	37.9	11.7	899.3
Unbiased Egalitr. Sampler	1, 4	5563.6	39.8	9.8	1016.2
Egalitarian Sampler	1, 3, 4	5333.8	40.3	0.6	856.1
Unbiased Sampler	1, 2, 4	5452.0	31.6	6.8	947.9
Mutation Sampler	1, 2, 3, 4	5304.7	26.9	-3.2	853.9

TABLE 2 AIC values of alternative models defined by dropping core principles of the mutation sampler.

ferences. Second, that such inferences are sometimes in error is attributed to the existence of cognitive resource limitations that restrict the number of samples taken (Principle 4). That such errors are systematic—that their pattern repeats across subjects and causal situations (as described below)—is attributed to the fact that sampling is biased to commence at certain network states (the prototypes) (Principle 3). It is also attributed to the fact that each subsequently sampled network state differs from the previous state by at most one variable (Principle 2).

The mutation sampler bears some similarities to past models of causal reasoning. For example, the mutation sampler is like *mental models theory* (MMT) (Johnson-Laird, 1980) in that it assumes that concrete possibilities (i.e., *models*) are represented and that some possibilities are more likely to be represented than others. It is also like Rehder's 2018 *beta-Q* model in proposing that people draw inferences on the basis of a non-normative joint distribution in which homogeneous prototype states are over-represented. Indeed, the mutation sampler can be viewed as a process level implementation of the principles embodied by beta-Q. In the General Discussion we compare the mutation sampler with these and other accounts of human causal reasoning.

3 | EMPIRICAL TESTS

We now assess the mutation sampler as an account of human causal judgments. Because our claim is that people generate samples of concrete states for multiple types of causal judgments, a key test of the mutation sampler is whether its predictions are borne out across a variety of causal reasoning studies. In particular, we assess fits of the mutation sampler to existing empirical datasets in reasoning, categorization, and intervention. To further test the task-generality of our model, we assess its fit to an entirely new task, one that asks subjects to make direct judgments of joint probability.

In each section the key comparison will be on the account of the empirical data provided by the mutation sampler as compared to the normative graphical model framework. A secondary goal will be to provide support not only for the mutation sampler but also for each of its four principles considered independently. To this end, we also discuss fits of not only the mutation sampler but also alternative sampling models in which one or more of those principles have been relaxed. For example, relaxing Principle 3 by starting to sample at a randomly chosen system state rather than one of the two prototype yields a model we will refer to as the *unbiased sampler*. Relaxing Principle 2 by using a proposal distribution in which all network states have equal probability of being selected as a proposal yields the *egalitarian sampler*. Relaxing both Principles 2 and 3 yields the *unbiased egalitarian sampler*. Because the Metropolis-Hastings rule embodied by the mutation sampler guarantees convergence to the true joint distribution, relaxing Principle 4 by stipulating unlimited sampling corresponds to the normative model. The results of these alternative models for each empirical section are summarized in Table 2.

Note that the general structure of these sections is to push most of the specifics about model fitting to appendices,

providing only high-level summaries of the relative performance of the models. This allows us to put a spotlight on illustrative examples showing why the mutation sampler achieves better fits than the alternative models, while still allowing motivated readers to delve into the particulars if they choose.

3.1 | Causal Reasoning

In a first empirical test of the mutation sampler, we assess how it accounts for conditional probability judgments that are drawn on the basis of causal knowledge. Appendix C presents fits of the normative model and the mutation sampler to 19 experimental conditions from four published articles, involving a total of 690 participants and 8 distinct causal network topologies. In every condition participants were first instructed on causal knowledge and then presented with a series of conditional probability queries, judgments in which participants estimate the probability that one variable is present given the state of one or more of the other variables.

For each participant, we fit versions of the normative model and the mutation sampler suitable for the causal network topology taught to that participant. For both models, those parameters included one representing the marginal probability of the variables that are root causes in a graph (e.g. Y_A and Y_B in Fig. 1), one representing the strength of every causal relation in the network, and one representing the strength of alternative causes (causes not explicitly part of the causal network itself), and a scaling parameter that scaled the predicted conditional probabilities onto the 0-100 rating scaled that participants used. The mutation sampler had an additional λ parameter representing mean chain length, that is, the mean number of samples taken. Details of the fitting procedure and the best fitting average parameter values are presented in Appendix C for each condition along with a number of measures of quality of fit.

Appendix C reveals that the mutation sampler yielded a better fit (according to a measure that corrects for the number of parameters, AIC) as compared to the normative model in every one of the 19 experimental conditions. In addition, a larger number of participants were better fit by the mutation sampler in 16 of the 19 conditions.

We briefly summarize the performance of the mutation sampler in two key conditions. First consider the three-variable common cause condition ($Y_A \leftarrow X \rightarrow Y_B$) in Fig. 4A. The Markov condition associated with causal graphical models and alluded to earlier stipulates that a variable is statistically independent of its non-descendents conditioned on the state of its immediate parents. Applied to the common cause graph, the Markov condition states that the two Y s should be independent conditioned on X , that is, the probability of one Y (call it Y_i) given the state of X should be unaffected by whether the state of the other Y (Y_j) is present, absent, or unknown. In other words, it should hold that $p(y_i^1|x^0y_j^0) = p(y_i^1|x^0) = p(y_i^1|x^0y_j^1)$ and $p(y_i^1|x^1y_j^0) = p(y_i^1|x^1) = p(y_i^1|x^1y_j^1)$.⁵ These predictions are represented by the two horizontal blue lines in Fig. 4A, which depicts the normative model's best fit to these data. The figure reveals that participants instead violated the conditional independence required by the Markov condition, judging that, for example, $p(y_i^1|x^1y_j^0) < p(y_i^1|x^1) < p(y_i^1|x^1y_j^1)$. This finding has been replicated in multiple studies (Ali et al., 2011; Lagnado & Sloman, 2004; Fernbach & Rehder, 2013; Mayrhofer & Waldmann, 2015; Park & Sloman, 2013; 2014; Rehder & Burnett, 2005; Rehder, 2014; 2018; Rottman & Hastie, 2016; Walsh & Sloman, 2004; see Hagmayer, 2016 or Rottman & Hastie, 2014 for review). Fig. 4A also reveals that those independence violations are reproduced by the mutation sampler. The independence violations predicted by the mutation sampler are a direct consequence of its biased starting points combined with a relatively small number of samples.

Second, for the three-variable common effect condition ($Y_A \rightarrow X \leftarrow Y_B$; Fig. 4B), the normative model stipulates that the two Y s should be unconditionally independent. That is, it should hold that $p(y_i^1|y_j^0) = p(y_i^1|y_j^1)$. This predic-

⁵Because of the symmetry of the two causal networks in Fig. 4 and the study's extensive counterbalancing of materials, we generally collapse over inferences involving variables that play interchangeable roles, such as Y_A and Y_B in Fig. 4. For example, the rating for the conditional probability judgment $p(y_i^1|x^1)$ shown in the figure is the average of $p(y_A^1|x^1)$ and $p(y_B^1|x^1)$, $p(y_i^1|x^1y_j^0)$ is the average of $p(y_A^1|x^1y_B^0)$ and $p(y_B^1|x^1y_A^0)$, and so forth.

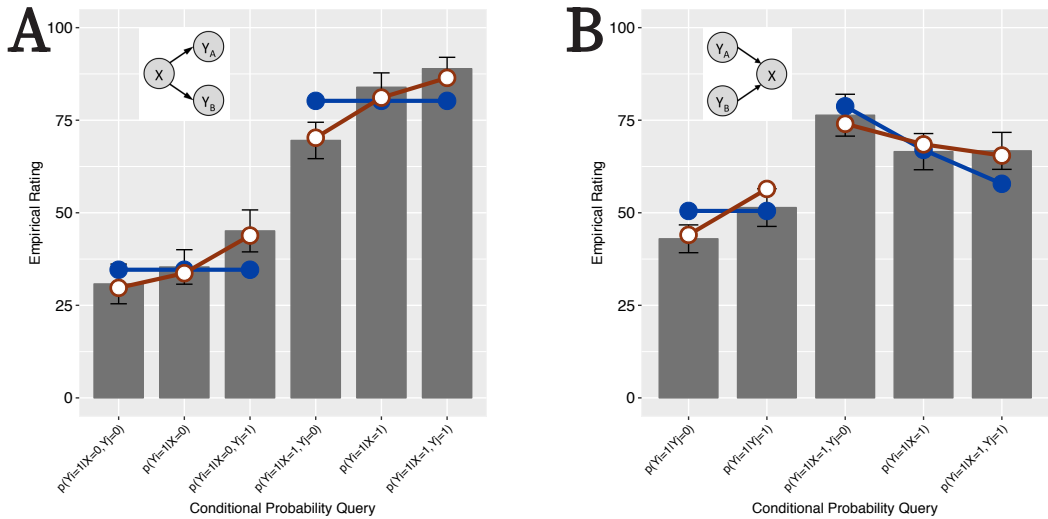


FIGURE 4 Data from Rehder and Waldmann (2017), Experiment 1. Fits of the mutation sampler (red lines, open plot points) and the normative model (blue lines, closed plot points) are superimposed on the empirical conditional probability judgments (gray bars). For example, in these studies participants judged the presence of the to-be-inferred variable on a 0-100 scale. Error bars denote 95% confidence intervals.

tion is represented by the horizontal blue line in Fig. 4B, the normative model's best fit to these data. Yet participants judged that $p(y_i^1|y_j^0) < p(y_i^1|y_j^1)$ instead. This apparent expectation that the causes of a common effect graph are positively correlated has been observed in other studies (Luhmann & Ahn, 2007; Perales et al., 2004; Rehder & Burnett, 2005; Rehder, 2014; 2015; 2018; Rottman & Hastie, 2016; Trueblood et al., 2017; cf. Von Sydow et al., 2010). Fig. 4B also reveals that the mutation sampler correctly accounts for this violation of independence.

The mutation sampler also accounts for another reasoning error that participants commit with the common effect graph in Fig. 4B. Explaining away is a signature property of common effect graphs with independent generative causes. If X is observed to occur then the probability that Y_i is present of course increases. But if it is then further observed that the other cause Y_j is present then the probability that Y_i is present should decrease back towards its baseline. Conversely, if Y_j is observed to be absent then the probability of Y_i should increase. That is, it should hold that $p(y_i^1|x^1y_j^0) > p(y_i^1|x^1) > p(y_i^1|x^1y_j^1)$. In fact however, research finds that participants often explain away too little or not at all (Morris & Larrick, 1995; Rehder, 2014; 2018; see Rottman & Hastie, 2014, for a review). The right three bars in Fig. 4B illustrate the three conditional probability judgments relevant to explaining away. The fits of the normative model to these data points reveal that explaining away with Rehder and Waldmann's participants was indeed too weak (the slope of the blue line is steeper than the empirical ratings). In contrast, the mutation sampler correctly predicts this too weak explaining away (the slope of the red line is shallower).

As indicated above, we also fit alternative versions of the mutation sampler in which one or more of the four principles were relaxed. The “Causal Reasoning” column in Table 2 presents the AIC values averaged over all conditions for the full set of models we tested. Recall that relaxing Principle 3 yields the unbiased sampler, relaxing Principle 2 yields the egalitarian sampler, relaxing Principles 2 and 3 yield the unbiased egalitarian sampler, and relaxing Principle 4 (i.e., engaging in unlimited sampling) or Principle 1 (avoiding sampling entirely) yields the normative model. Table 2 indicates that the mutation sampler yields a fit that is not only better than the normative model but also better

than each of the alternative sampling models that do not implement all four principles. The supplementary materials presents an example of how each of the four principles independently contribute to the success of the mutation sampler by presenting the fits of each sampling model to one particular data set.

3.2 | Causal Categorization

As mentioned, the design of the mutation sampler was partly inspired by the need to explain prominent failures in human causal reasoning, such as independence violations and weak explaining away. Having shown that it succeeds at this task, the next two sections ask whether its predictions generalize to alternative kinds of causal judgments. In this section, we assess how the mutation sampler accounts for categorization judgments drawn on the basis of causal knowledge.

Appendix D presents fits of the normative model and the mutation sampler to 25 experimental conditions from 7 published articles, involving a total of 1044 participants and 9 distinct causal network topologies. In every condition participants were instructed on novel categories whose features were causally related. For example, some participants were informed of a type of star named Myastars with binary dimensions such as type of helium (ionized or not), density (high or normal), number of planets (large or normal), and so forth. The generative causal relations were described as one feature causing another (e.g., ionized helium causes a large number of planets). After learning their assigned category participants were presented with test items with features and asked to rate on a 0-100 scale the likelihood that each was a member of the category.

We fit versions of the normative model and the mutation sampler suitable for the causal network topology in each experimental condition. Because the materials were categories, their description included information specifying that one feature on each binary dimension was more prevalent than the other. For example, in one study, participants were told that "Most Myastars have high density whereas some have normal density." Because of these uneven base rates, we granted the mutation parameter the additional *bias* parameter described above that controls the probability that sampling process starts at the prototype state with all 1s versus the one with all 0s.

Details of the studies and fitting procedure are presented in Appendix D, along with the best fitting parameters and measures of fit. It reveals that the mutation sampler yielded a better fit (correcting for the number of parameters) as compared to the normative model in 21 of the 25 experimental conditions. Fig. 5 presents categorization queries from three of those conditions, which again superimposes the fits of the normative model and mutation sampler on the empirical ratings. Note that the values of the fitted bias parameter was greater than 0.5 in the large majority of studies, suggesting that it indeed reflected the fact that one feature on each dimension was considered characteristic of the category and the other was uncharacteristic.

Fig. 5A presents the categorization ratings associated with a common effect network with three cause features. The eight distinct types of categorization test items presented in the figure are organized into two groups of four. The group on the left includes the test items in which the common effect X is absent. As the number of Y s that are present increases from zero to three, categorization ratings decrease, because more Y s means more violations of the causal relations. The group on the right includes the test items in which X is present. For these items ratings increase with more Y s because more causal relations are confirmed (and, generally, because more characteristic features makes for a better category member). Although the normative model (blue lines, closed plot points) accounts for this qualitative pattern, it underestimates the joint probability of the two prototypes ($y_A^0 y_B^0 y_C^0 x^0$ and $y_A^1 y_B^1 y_C^1 x^1$; see outer bars in the figure) and slightly overestimates the states in between. In contrast, the mutation sampler (red lines, open plot points) yields a better account of these data, including the two prototypes.

Fig. 5B presents results from a three feature causal chain. From left to right, the eight test items are organized

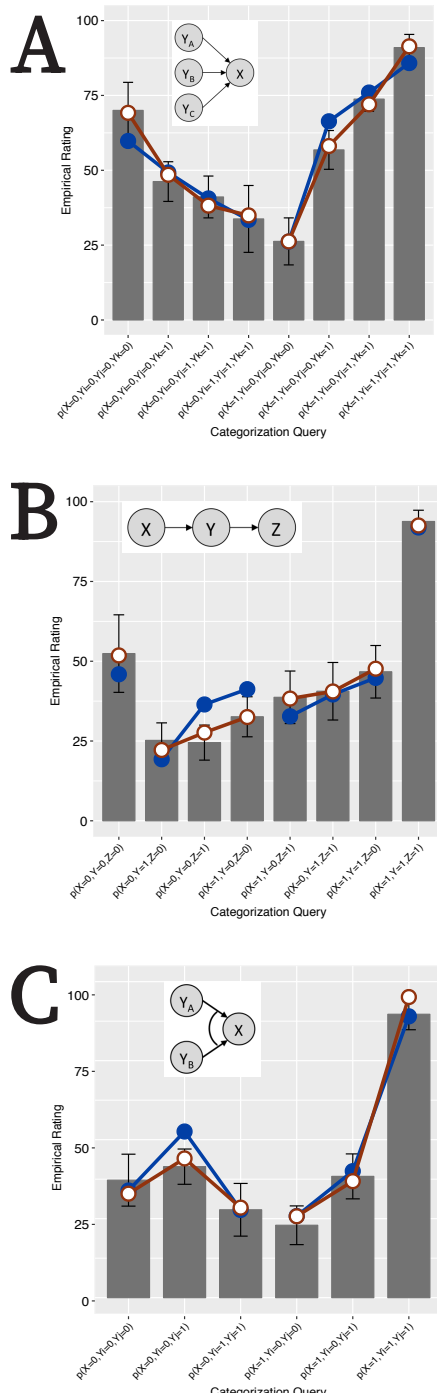


FIGURE 5 Categorization data from (A) Rehder (2003a), common effect condition; (B) Rehder and Kim (2010), Experiment 1, weak condition; and (C) Rehder (2015), Experiment 1, conjunctive condition. Fits of the mutation sampler (red lines, open plot points) and the normative model (blue lines, closed plot points) are presented superimposed on the empirical data (gray bars). Error bars denote 95% confidence intervals.

into (a) the $x^0y^0z^0$ prototype, (b) the three items in which one feature is present, (c) the three in which two features are present, and (d) the $x^1y^1z^1$ prototype. Within both the one-feature and two-feature items, the items on the left ($x^0y^1z^0$ and $x^1y^0z^1$) violate two causal relations whereas the other members of each group violate only one. Although participants' ratings reflect this difference in the number of violated causal relations, the panel makes clear that they do not do so to the degree predicted by the normative model. In contrast, the mutation sampler reproduces these ratings because it reduces differences in the joint probability of non-prototype items.

Fig. 5C presents results from a common effect network with two features that are a conjunctive cause of a third. The six types of test items are organized into two groups. X is absent in the group on the left and present in the one on the right. When X is absent, the normative model predicts that the joint probabilities will increase with the introduction of the first Y cause feature but then sharply decrease with the introduction of the second, because when both Y s are present the absence of X represents a violation of the (conjunctive) causal relation. Participants ratings reflected this pattern, but less sharply than the normative model. The mutation sampler, in contrast, reproduced participants' ratings.

The "Causal Categorization" column in Table 2 presents the AIC values averaged over the 25 experimental conditions to not only the normative model and the mutation sampler but also each of the alternative sampling models. Once again, we found that the mutation sampler yielded the best fit. That its fit was superior to the normative model provides support for the sampling approach to causal categorization (Principles 1 and 4). That it was superior to the alternative sampling models supports a proposal distribution that only proposes states that differ by one variable (Principle 2) and that sampling begins at the prototypes (Principle 3). The supplementary materials presents fits of each sampling model to one particular data set.

3.3 | Causal Interventions

The third type of task we aim to account for is causal interventions. Whereas in a typical causal inference a reasoner observes the states of one or more variables and then predicts the state of another variable, in an intervention the reasoner is asked to imagine that an agent external to the causal system has acted on the system so as to set one of the variables to a particular state. Causal graphical models stipulate that valid inferences depend on whether variables are observed or intervened upon.

Consider the two causal models tested by Waldmann and Hagmayer (2005, Experiment 1) shown above Fig. 6I. Participants were told they were being instructed on a sleeping sickness in which a mosquito bite causes the production of a substance named pixin. In one condition, participants were taught the causal relations between *pixin* (P) and *xanthan* (X), *sonin* (S), *gastran* (G), and *histamine* (H) depicted by Model A in Fig. 6I. In another they were taught Model B, which is identical to Model A except that the direction of the causal relationship between X and G is reversed. All participants then observed training data consisting of 20 patients and their values on each of the five variables. This data reflected deterministic causal relations (a cause was always accompanied by its effect) and a base rate for P of 0.5. Participants then predicted the state of S given the state of H in a particular patient. Whereas in the observation condition participants merely observed H to be high (or low), in the intervention condition they were told that a doctor had inoculated the patient with a substance that raises (or lowers) the level of H (such interventions are depicted by a double-lined arrow in Fig. 6I and are denoted $do(h^i)$).

The importance of the state of H being due to an intervention is that an inference from H to P is no longer licensed. According to the logic of *graph surgery* (Pearl, 2000), an intervention on H can be modeled by the removal of the $P \rightarrow H$ causal relation (depicted by a dashed line in Fig. 6I). Thus, the difference between the observation and intervention condition is that whereas H provides information about S in either condition in Model B (via the path

$H - G - X - S$, it does so only in the observation condition in Model A (the $H - P - X - S$ path is blocked when H is intervened upon).

As was the case for the previous judgment types, we also fit the alternative sampling models to these experiments. The “Causal Intervention” column in Table 2 indicates that once again the mutation sampler yielded a better fit than not only the normative model but also each of the alternative sampling models (see the supplementary materials for the fits of each model to Waldmann and Hagmayer’s Experiment 1).

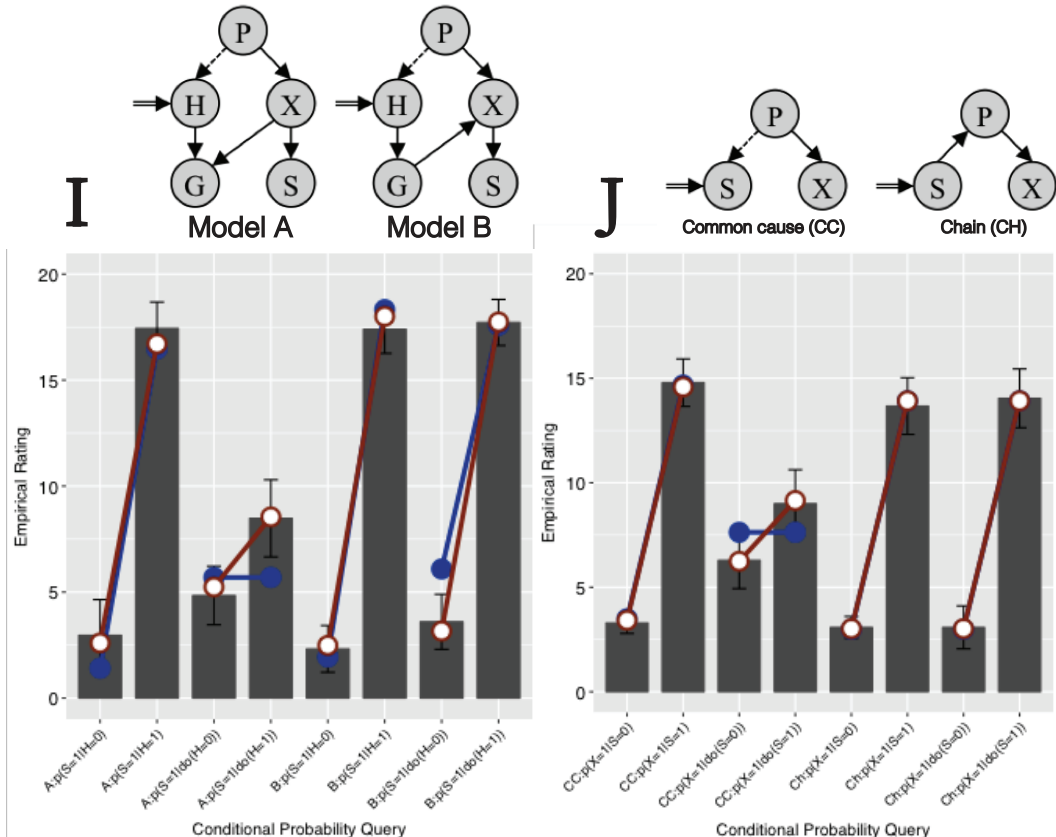


FIGURE 6 Intervention data from Waldmann and Haggmayer (2005), Experiments 1 (panel I) and 2 (panel J). Double-lined arrows indicate interventions.

The empirical results from Waldmann and Haggmayer’s (2005) Experiment 1 are shown in Fig. 6I. The four inferences with Model A (H = high vs. low crossed with H observed or intervened upon) are shown on the left and those with Model B are shown on the right. For Waldmann and Haggmayer’s purpose, the important finding was that participants judged H to be highly diagnostic of S in Model B regardless of whether H was observed or intervened upon, whereas for Model A H was regarded as diagnostic of S when H was observed, but not when it was intervened upon. This result highlighted the fact that reasoners are in fact quite sensitive to the different inferences that are licensed when a variable is intervened upon rather than observed. For our purpose, the important finding is that whereas the

difference between $p(s^1 | do(h^1))$ and $p(s^1 | do(h^0))$ in Model A was indeed modest, it was clearly greater than zero. This is the case despite the fact that H and S are conditionally independent in Model A after the surgery that removes $P \rightarrow H$. That is, from the perspective of the normative causal graphical model framework, the results in Fig. 6J represent another form of independence violation.

To illustrate the performance of the mutation sampler in this context, we fit it (red lines, open plot points) and the normative model (blue line, closed plot points) to the aggregated ratings in each experimental condition. For the mutation sampler, we assume that sampling occurs over the graphs in Fig. 6 in the observation conditions but that it occurs over the post-surgery version of those graphs (i.e., the dashed arrows are removed) in the intervention conditions. (See Appendix E for additional details regarding the fitting procedure.). Fig. 6I shows that both models account for most data points. But whereas the normative model is constrained to predict $p(s^1 | do(h^1)) = p(s^1 | do(h^0))$, the mutation sampler correctly predicts that $p(s^1 | do(h^1)) > p(s^1 | do(h^0))$.

Fig. 6J presents the results from Experiment 2 from Waldmann and Hagmayer (2005). As was the case for Models A and B in Fig. 6I, the common cause and chain models tested in this experiment license the same qualitative inferences under observation but not under intervention (in this experiment, variable S was observed or intervened upon and X was the to-be-predicted variable). In particular, whereas the normative common cause model predicts $p(x^1 | s^1) > p(x^1 | s^0)$, it also predicts $p(x^1 | do(s^1)) = p(x^1 | do(s^0))$ because of the surgery that removes $P \rightarrow S$ causal relation. But although participants' inferences again showed that they were quite sensitive to observations versus interventions, they incorrectly judged that $p(x^1 | do(s^1)) > p(x^1 | do(s^0))$. The fits in Fig. 6J superimposed on the empirical ratings show that this independence violation can be accounted for by the mutation sampler but not the normative model. Note that unlike the first experiment, the data accompanying the causal models implied causal links that were quite strong but not deterministic, demonstrating that independence violations in the context of interventions are not limited to deterministic relations. Just as with the previous data sets, the mutation sampler yielded a better fit than not only the normative model but also the three alternative sampling models (Table 2).

4 | CAUSAL REPRESENTATIONS

One key aspect of the empirical results presented thus far is that the mutation sampler accounts for not only a large number of experimental conditions and participants but also different types of causal judgments. This result lends support to our assumption that the samples generated by mutation sampling serve as the basis for many judgment types and that the small but systematic distortions introduced by that sampling will therefore manifest themselves on multiple tasks. Our final empirical test of the mutation sampler involves a novel methodology that provides a relatively direct assessment of participants' beliefs about the relative likelihood of the states of a causal graph. We ask whether the distortions introduced by mutation sampling – distortions we have implicated as the source of the reasoning errors in the previous sections – can be observed directly in participants' own generated samples.

4.1 | Method

4.1.1 | Materials

Participants were presented with causal graphs in one of three domains: meteorology, sociology, or economics. Each domain had three variables (in economics: interest rates, trade deficits, and retirement savings; in meteorology: ozone levels, air pressure, and humidity; in sociology: urbanization, interest in religion, and socioeconomic mobility). Each variable could take on two possible values. One of these values was described as "Normal" and the other was either

"High" or "Low". The values of the variables were mixed to prevent domain-specific beliefs from affecting the results (alternate values were either all "High", all "Low", or a mixture of "High" and "Low"). For half of the participants the causal relations on which they were instructed formed common effect graph ($Y_A \rightarrow X \leftarrow Y_B$), whereas for the other half they formed a common cause graph ($Y_A \leftarrow X \rightarrow Y_B$). Each causal relationship was expressed as the High (or Low) value of one variable causing the High (or Low) value of another. For example, in the domain of economics one of the causal relationships was "Low interest rates cause small trade deficits. The low cost of borrowing money leads businesses to invest in the latest manufacturing technologies, and the resulting low-cost products are exported around the world." (No information was given about the relations between the "Normal" values of the variables.) See Rehder (2014) for additional examples of the causal relations.

4.1.2 | Procedure

Each participant was instructed on either a common cause or a common effect graph. Participants first studied screens of information that defined the variables, presented verbal descriptions of each causal relation (including the mechanism via which a cause could independently generate the effect), and a diagram of the causal relationships. Participants were then required to pass a multiple-choice test of this knowledge that ensured they knew which variables were causally related and the direction of those relationships.

Next, participants were asked to generate a data set that they would expect to result from the causal graph. The causal relationship between smoking and lung cancer was used as an example. Participants were shown the four cells formed by crossing smoker/non-smoker with lung cancer/no-lung cancer and how (in terms of how hypothetical people were allocated to the four cells) a greater proportion of smokers had lung cancer as compared to non-smokers. Participants were asked to generate an analogous distribution in their assigned domain (economics, etc.). Specifically, they were given 50 U.S. pennies and asked to distribute them among the cells formed by crossing the three binary variables. They did so by placing the coins on a large sheet that contained the eight possible states (the position of the states on the sheet was randomized).⁶

4.1.3 | Design and Participants

The experiment consisted of a 3 (domain) by 4 (variable states, e.g., all "High") by 2 (network structure, i.e., common cause or common effect) between-participants design. 120 New York University undergraduates received course credit for participation.⁷

4.2 | Results

Initial analyses revealed no effect for domain or variable states, so the results were collapsed over these factors. As expected, the allocation of coins differed depending on whether participants were instructed on a common cause or common effect graph and thus the results from these two conditions are presented separately.

⁶In particular, for each of the three domains there were four alternate value configurations (all "High"; all "Low"; two "High" and one "Low"; and one "High" and two "Low"). For each of these twelve counterbalanced conditions, there were two separate sheets with the position of the concrete cases on the sheet randomly assigned (resulting in a total of 24 sheets).

⁷This study was approved by the New York University Institutional Review Board under protocol number IRB-FY2017-68.

4.2.1 | Common Effect Condition

Fig. 7A presents how participants allocated the 50 coins to the eight states of a common effect graph (gray bars), states depicted in the original Fig. 1A. First note that these allocations indicate that participants judged that the two prototype states ($y_A^0 y_B^0 x^0$ and $y_A^1 y_B^1 x^1$), shown on the far left and far right of Fig. 7A, respectively, were the most probable whereas the rest of the states were less probable. This result was expected and indicates that participants attended to the causal relations they learned. However, the important theoretical question is whether their distributions of coins reflects the kinds of distortions relative to the normative model predicted by the mutation sampler. To answer this question, Fig. 7A also presents the best fits of both the normative model (blue line, closed plot points) and the mutation sampler (red line, open plot points) superimposed on the empirical data.⁸ Note that, relative to the normative model, the mutation sampler overpredicts the number of coins for the two prototype states and underpredicts the remaining states, a pattern that of course reflects the theoretical predictions presented earlier in Fig. 3A. More importantly, the figure makes clear that participants' distributions of coins were better accounted for by the mutation sampler. Indeed, a measure of fit that corrects for the difference in the number of parameters in the two models (AIC) confirmed that the mutation sampler yielded a better fit as compared to the normative model (AIC of 793.4 vs. 993.2).

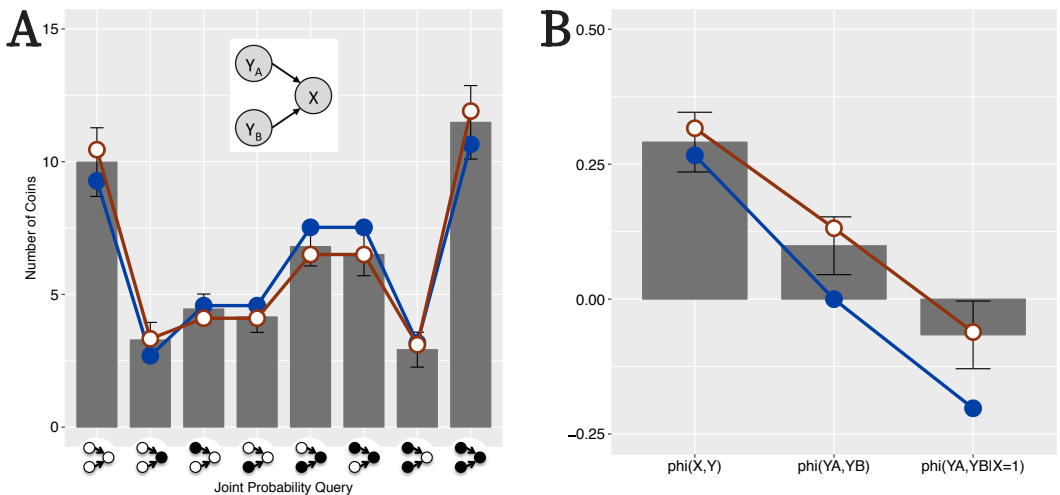


FIGURE 7 Results from the common effect condition. (A) Fits of the mutation sampler (red line, open plot points) and normative (blue line, closed plot points) are presented superimposed on participant's distribution of coins (gray bars). (B) Phi coefficients derived from participant's judgments in the common effect condition along with those derived from corresponding mutation sampler and normative model fits. Error bars denote 95% confidence intervals.

We also wanted to relate the results in Fig. 7A to the findings reported earlier regarding how people answer conditional probability queries. To do so we derived measures that reflect the statistical relationships among the three variables implied by a participant's distribution of coins. In particular, we first normalized that distribution and then computed the phi coefficient between a Y and an X , $\phi(Y_i, X)$ (the coins were aggregated so that the two Y s

⁸The best fitting parameters were those that maximized the likelihood of the normalized distribution of coins. Averaged over participants, those parameters were $c = .519$, $m = 0.440$, and $b = .243$ for the normative model and $c = .534$, $m = 0.410$, $b = .328$, and $\lambda = 10.1$ for the mutation sampler. To make them comparable to participants' distribution of coins, in Fig. 7A the models' fits have been multiplied by 50.

are interchangeable), between the Y s themselves, $\phi(Y_A, Y_B)$, and between the Y s conditioned on the presence of X , $\phi(Y_A, Y_B|x^1)$. These measures averaged over participants are presented in Fig. 7B. First note that the fact that $\phi(Y_i, X) \gg 0$ indicates that participants distributed the coins in a manner that reflected positive correlations between the Y s and X and thus their understanding that the Y s were generative causes of X . Of greater theoretical importance is the fact that $\phi(Y_A, Y_B)$ was also significantly greater than 0, $t(59) = 3.62, p < .001$. That is, the positive correlation between the causes of a common effect graph, observed earlier in people's causal inferences (see Fig. 4B) and representing an independence violation, also manifested itself in their distribution of the coins. Finally, note that $\phi(Y_A, Y_B|x^1)$ is significantly less than 0, $t(59) = -2.07, p < .05$. That is, the negative correlation between the causes conditioned on the presence of the common effect observed earlier in people's explaining away inferences (Fig. 4B) also manifested itself in their distribution of coins.

To directly assess the models' ability to account for these effects, we also derived the phi coefficients implied by their fits to the distributions of coins. These coefficients are superimposed on the empirical phi coefficients in Fig. 7B. As expected, the normative model, which stipulates that the Y s are independent (i.e., that $\phi(Y_A, Y_B) = 0$), is unable to account for the fact $\phi(Y_A, Y_B) > 0$. And although the normative model correctly predicts that $\phi(Y_A, Y_B|x^1) < 0$, it sharply overestimates the magnitude of that effect. Once again, we see that the mutation sampler but not the normative model accounts for the independence violations and the too-weak explaining away exhibited by human reasoners.

4.2.2 | Common Cause Condition

Fig. 8A presents how participants allocated the 50 coins to the eight states of a common cause graph. Fig. 8A presents the fits of the normative model and the mutation sampler these data.⁹ Although the mutation sampler achieved a better fit than the normative model (sum of squared error of 17.5 vs. 25.0), that improvement was not sufficient to yield a better fit for the mutation sampler correcting for its extra parameter (AIC of 914.4 vs. 805.4).

Nevertheless, just as in the common effect condition we derived statistical measures characterizing the joint, which are presented averaged over participants in Fig. 8B. That $\phi(X, Y_i) \gg 0$ (i.e., that X was viewed as positively correlated with the Y s) indicates that participants understood that X was a generative cause of the Y s. That $\phi(Y_A, Y_B) \gg 0$ (i.e., that the Y s were viewed as positively correlated with each other) indicates that participants correctly understood that, in a common cause graph, one Y predicts another. The final coefficient in Fig. 8B, $\phi(Y_A, Y_B|X)$, represents the degree to which the Y s were viewed as positively correlated conditioned on X .¹⁰ The Markov condition associated with causal graphical models of course stipulates that the Y s are independent conditioned on X , that is, that $\phi(Y_A, Y_B|X) = 0$. Participants in this condition judged instead that $\phi(Y_A, Y_B|X) > 0$, $t(59) = 3.60, p < .001$. That is, the violation of independence between two effects supposedly screened off by their common cause, observed earlier in people's causal inferences (Fig. 4A), is also observed here in their distributions of the coins. The phi coefficients derived from the model fits in Fig. 8B shows that the mutation sampler but not the normative model can account for the fact that $\phi(Y_A, Y_B|X) > 0$.

As in the previous sections, we fit the alternative sampling models to both the common cause and common effect conditions. Table 2 indicates that the mutation sampler yielded a better fit than the alternative sampling models. The Supplementary Materials presents fits of each sampler to the current common effect condition.

⁹The best fitting parameters for the normative model were $c = .510, m = .556$, and $b = .285$. Those for the mutation sampler were $c = .472, m = .466, b = .323$, and $\lambda = 8.3$.

¹⁰ $\phi(Y_A, Y_B|X)$ was computed as the average of the cases where X was present, $\phi(Y_A, Y_B|x^1)$, and absent, $\phi(Y_A, Y_B|x^0)$.

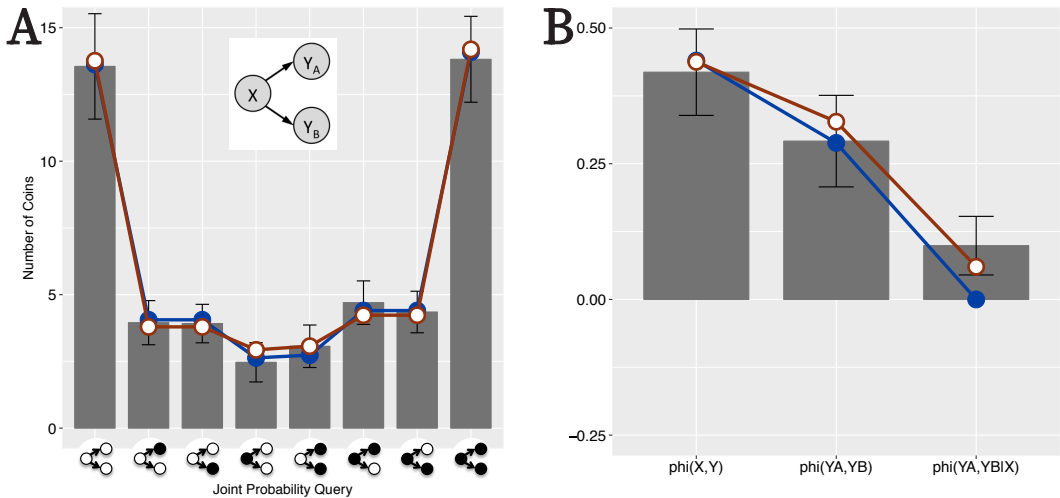


FIGURE 8 Results from the common cause condition. (A) Fits of the mutation sampler (red line, open plot points) and normative (blue line, closed plot points) are presented superimposed on participant's distribution of coins (gray bars). (B) Phi coefficients derived from participant's judgments in the common effect condition along with those derived from corresponding mutation sampler and normative model fits. Error bars denote 95% confidence intervals.

4.2.3 | Discussion

The results of this experiment confirm that the distortions introduced by mutation sampling—distortions we have implicated as the source of the errors that obtain during causal reasoning, categorization, and interventions—can be observed directly in participants' own generated samples. We do not wish to claim that the mental processes invoked by a task that requires explicit construction of a causal sample corresponds exactly to those involved in these earlier judgments. Nonetheless, it is striking that the distributions that participants judged to be representative of causal graphs exhibited the same statistical properties—dependence violations and weak explaining way—shown earlier. That the phenomena predicted by the mutation sampler manifest themselves on such a variety of judgments suggests that it has implications not just for specific tasks but for causal cognition more generally.

5 | GENERAL DISCUSSION

Although causal graphical models have enjoyed success in modeling causal cognition, less work has investigated the cognitive processes by which such sophisticated judgments are made. We have introduced a rational process model that generates samples from a causal system upon which many causal-based judgments can be based. Overall, we found that the mutation sampler yielded a better fit across a diverse array of experimental conditions that tested a large number of participants. First, we found that the mutation sampler provided a better account of conditional reasoning judgments, a heavily studied task within the causal graphical model framework. We then assessed the performance of the mutation sampler on two additional tasks—categories with causal structure and interventions. Past work has emphasized the success of causal graphical models in these domains but we showed that the biases to joint distributions induced by mutation sampling also manifest themselves on these additional judgment types. Finally,

we confirmed the predictions of the mutation sampler using a new methodology that assessed, in a relatively direct way, people's causal representations.

The mutation sampler instantiates four key principles of the process of drawing causal inferences, all of which are necessary to reproduce people's judgments. Principle 1 is that people reason about concrete cases, rather than directly instantiating a full joint distribution. Dropping this principle would involve exact Bayesian inference, which we have shown does not match people's judgments. Principle 2 states that people only make small adjustments to the concrete cases that they are considering. We showed that a sampling model that relaxes Principle 2—the egalitarian sampler—was unable to fully fit people's causal judgments. Principle 3 stipulates that people begin sampling from prototype states. A model without this principle—the unbiased sampler—also did not account for subjects' causal judgments as well as the mutation sampler. Finally, Principle 4 proposes that people have limited cognitive resources and thus take some small number of samples. Because the mutation sampler asymptotically approaches the normative joint distribution, dropping Principle 4 would result in behavior indistinguishable from the normative model (and therefore poorly matching people's behavior).

Below we first consider some of the properties of a sampling approach to causal reasoning. We first discuss alternative sampling algorithms and the constraint of cognitive efficiency that any process model is obligated to satisfy. The mutation sampler is then compared to some alternative accounts of causal reasoning. We then consider some phenomena in causal cognition that are unaddressed by computational level models (such as causal graphical models) but potentially explainable by a process model such as the mutation sampler, including the variability in causal judgments, individual differences, and reaction times. We close with a discussion of generalizations to the mutation sampler to causal scenarios that have received relatively less empirical study.

5.1 | Summary of Sampling and Causal Inference

5.1.1 | Other Sampling Algorithms

Earlier we noted that there are other possible sampling algorithms that would behave similarly to our model. For example, the mutation sampler shares many similarities with another Markov Chain Monte Carlo algorithm: the Gibbs sampler (Casella and George, 1992). The Gibbs sampler operates by selecting a single node to resample according to its conditional probability given the values of all other nodes. This process is similar to the mutation sampler's selection of a single node to flip and comparison of the probability of the two states. The most common form of Gibbs sampler is a *block* Gibbs sampler, where all nodes are sequentially resampled to get the new state. However, we make a slight modification to the Gibbs sampler by updating the state after each resampling, and not requiring that all nodes are resampled in turn. This small adjustment to a Gibbs sampler, along with initializing it at the prototype states, implements all four of our key principles: concrete cases, limited sampling, biased starting points, and a 'neighbors' proposal distribution.¹¹

We fit our altered Gibbs sampler to the conditional probability and categorization data from Sections 3.1 and 3.2, and found remarkably similar results, from quality of fit to parameter estimates such as causal strength (details available from the authors). In fact, the two models exhibited consistent variation from each other only in the number of samples required to fit people's behavior. The mutation sampler was able to fit participant's judgments with fewer samples than the Gibbs sampler, a result of the increased efficiency of the MH sampling algorithm. Although the data as it stands cannot distinguish between these two models, both are clearly preferred over the normative model. For

¹¹While the two models share many commonalities, they are not identical. The transition probabilities the modified Gibbs sampler defines, $a(q'|q) = \pi(v'_i|u_i)$, are distinct from those of the mutation sampler, $a(q'|q) = \min(1, \pi(v'_i|u_i)/\pi(v_i|u_i))$.

this reason we take these findings as support for our key principles, regardless of choice of the particular MCMC algorithm.

5.1.2 | Efficiency

As mentioned, we believe that people generally exhibit an impressive ability to reason causally, a fact that explains why the causal graphical model framework has enjoyed success in modeling causal cognition. Any process model purported to account for this phenomenon is therefore constrained to postulate cognitive mechanisms whose resource demands are within reach of most human reasoners for most causal based judgments. For this reason we believe it is important to emphasize again that the mutation sampler constructs samples in a manner that is computationally efficient and so psychologically plausible. The Metropolis-Hastings rule combined with the proposal distribution we advocate requires computing the relative likelihood of two graph states that differ by one variable, excluding variables not in the variable's Markov blanket. Appendix A demonstrated that this computation can be reduced to simple expressions involving the probabilities that define how variables are generated from their parents, probabilities that are assumed to already be explicitly represented as part of a causal graphical model.

Another aspect of efficiency of course concerns the size of the representations that are required. A well-known advantage of causal graphical models is that, by only encoding the local dependencies between variables and their parents, they avoid the exponential explosion in the space required if causal systems were represented as full joint distributions. Of course, the purpose of the mutation sampler is to approximate that joint distribution, which raises the question of whether drawing inferences via sampling reintroduces the problem of unrealistic space requirements that causal graphical models were intended to solve in the first place. However, note that sampling needs to represent not all network states but rather only those that are visited (i.e., sampled). For example, if one runs the mutation sampler on the five variable graph of Fig. 2 (which has $2^5 = 32$ distinct states) with chain lengths of 6, 12, 24, and 36 under the same parameterization specified in Appendix A, the average number of distinct network states that are actually sampled are 2.9, 4.9, 7.8, and 10.0, respectively. This exercise reveals that a psychologically plausible amount of sampling is accompanied by psychologically plausible memory requirements. Later we will provide evidence that the small number of sampled network states results in variability that qualitatively matches that of participants.

Additional efficiencies are possible depending on the type of judgment a reasoner is faced with. Although the approach here has been to use the mutation sampler to estimate a joint distribution, which is then used to derive predictions for a specific task, the full joint distribution is often unnecessary. For example, when estimating a conditional probability, sampling the part of a causal network's state space in which the query's antecedent is false is a waste of cognitive resources. To investigate this opportunity for further optimization, we defined an alternative version of the mutation sampler. Whereas in the mutation sampler's proposal distribution each mutated state has an equal chance of being proposed, in the alternative sampler those network states in which a conditional probability query's antecedent is true are ten times more likely to be proposed than those in which it is false. This modification means that sampling is strongly biased towards that part of the network's state space needed for the computation of that conditional probability. Appendix F confirms that, for the network in Fig. 2, the rate at which conditional probability queries estimated via sampling converge to the true conditional probabilities is faster for this alternative sampler as compared to the standard mutation sampler. Indeed, for those particular queries the average accuracy achieved by the mutation sampler in 12 samples was matched by the alternative sampler after only 5.8 samples. Of course, computing conditional probabilities via sampling is also highly space efficient, because one need not remember visited network states at all. Rather, one only need keep a tally of the number of visited states that satisfy the antecedent and, of those, the number that satisfy the consequent (and then divide the latter by the former).

We have assumed throughout that reasoners generate a new chain of samples in response to each causal-based query, a strategy especially appropriate for “one shot” (non repeated) causal judgments. However, when a number of such judgments are posed in close temporal proximity (as in the typical causal reasoning experiment), the samples generated for old judgments could potentially be reused to answer new ones. Indeed, one conjecture is that sampling is common early in an experimental session but gradually becomes less common as judgments start being made on the basis of (possibly an aggregation of) previous samples stored in memory. Responding on the basis of stored chains of samples would be another potential sources of efficiency, and there is evidence that people use amortization in some judgments (Dasgupta et al., 2018). On the other hand, sharing chains across causal queries will be less likely if, as described above, those chains are generated in a manner that is specific to each query (e.g., are constrained to be consistent with the antecedent of a conditional probability query).

5.2 | Alternative Models

5.2.1 | Beta-Q

As alluded to earlier, one model that shares some important similarities with the mutation sampler is Rehder's (2018) *beta-Q* model. Like the mutation sampler, beta-Q proposes that people draw inferences on the basis of non-normative joint distributions and, moreover, that it is the homogeneous “prototype” states that are over-represented in those distributions. That the joints defined by the two models share these properties of course means that they make many of the same predictions. For example, both models not only predict the basic independence violations and weak explaining away results documented by numerous investigators (e.g., those shown earlier in Fig. 4), but also some newer phenomena reported in Rehder (2018), such as the fact that independence violations arise even when causal inferences are screened off by three variables. In fact, the data sets from Rehder (2018) comprised six of the causal reasoning conditions successfully fit by the mutation sampler and one particular result from that study was cited as support for the mutation sampler's proposal distribution (see Appendix C).

However, an important difference between the models is that whereas beta-Q is a descriptive account, we advocate the mutation sampler as a process level account of the mental operations that underlie causal judgments. For example, the distortions to a normative joint distribution stipulated by beta-Q were defined in terms of *energy functions* that were, in essence, added to a normative joint in order to achieve the needed distortion. But although beta-Q replicated participants' behavior, it provides no explanation of why joint distributions are distorted in that manner (or at all). In contrast, the mutation sampler provides an explanation for why those distributions might arise, namely, as a result of a mental sampling process that is limited and constrained to commence at certain easily imagined network states. For these reasons, we believe that the mutation sampler can be viewed as the process level implementation of the computations specified by beta-Q.¹² Of course, as a process model the mutation sampler has the potential to also account for some of the behaviors we discuss below (e.g., reaction times) that are outside the purview of descriptive models like beta-Q.

¹²The beta-Q model includes a parameter q that determines the degree of distortion to the joint distribution, where larger distortions are implied by large values of q (and no distortion is implied when $q = 0$). Thus, q is inversely related to the chain length defined by the mutation sampler (where longer chain lengths imply more veridical joint distributions). In fact, we have established that chain lengths in the range [2, 7] yield causal inferences that are virtually identical to those generated by beta-Q with q in the range [1.33, 0.50]

5.2.2 | Quantum Probability Models

Recently, Trueblood et al. (2017) applied *quantum probability theory* (QP) to some of the causal reasoning phenomena considered here. Whereas in classic probability theory probabilities are computed as subsets (of a joint probability distribution), in QP events are represented as subspaces and probabilities are computed by taking the inner product of vectors within those spaces. One key factor that determines QP probabilities is the *dimensionality* of the representational space deemed appropriate for a domain. When all N (binary) domain variables are *compatible*, then the dimensionality of the space is 2^N and QP can yield classic probabilities. But *incompatible* variable pairs result in a reduction in dimensionality (to 2 in the extreme case in which all pairs are deemed incompatible). This reduction addresses the exponential growth in space requirements alluded to above but at the cost of introducing so-called *quantum effects*, probabilities that do not necessarily honor the properties of classic probability theory. For example, QP interprets conjunctive probabilities in terms of a sequence of vector operations. Because $p(X, Y)$ and $p(Y, X)$ involve distinct sequences of such operations, in low dimensionality spaces commutativity in which $p(X, Y) = p(Y, X)$ need not hold.

One strength of QP is that it provides a natural account of order effects. For example, if $p(Z|X, Y)$ is interpreted as $p(Z|X \text{ then } Y)$ (i.e., one first learns that X and then that Y), then QP potentially accounts for the finding that the order of X and Y matters (i.e., that $p(Z|X \text{ then } Y) \neq p(Z|Y \text{ then } X)$). In fact, Trueblood et al. (2017) found order effects in a causal reasoning task such that more recently presented information was weighed more heavily (also see Trueblood & Busemeyer, 2012). They also found that appropriately parameterized QP models could reproduce Markov violations and weak explaining away, phenomena we have taken here as evidence for the mutation sampler.

Although QP is a potentially important contribution to the understanding of human probabilistic reasoning, as presently formulated its application to causal reasoning is incomplete. Thus far, QP has only been applied to one causal network topology (a three-variable common effect network, Trueblood & Busemeyer, 2012; Trueblood et al., 2017). More generally, no principles have been specified that determine which variables in a causal network should be treated as compatible or incompatible (and thus the dimensionality of the space) as a function of their causal roles. As a result, QP makes no *a priori* predictions regarding how, for example, judgments should differ between a common effect and a common cause network. The asymmetries in human judgments elicited by these two network topologies have provided key evidence in favor of the causal graphical model framework. Similarly, within a QP space no principles guide the values of free *rotation parameters* (that determine the relations between the basis vectors that represent incompatible variables) as a function of, say, the strengths of the causal relations (and thus QP makes no *a priori* predictions that stronger causal relations should support stronger inferences). Finally, and most importantly for present purposes, QP is fundamentally a descriptive model of the causal reasoning phenomena investigated here. Just like beta-Q, QP specifies computations that are intended to reproduce human causal inferences without specifying how those computations are carried out. In contrast, the goal of the mutation sampler is to describe not only what causal inferences people draw but also how they do it.

5.2.3 | Mental Models Theory

The mutation sampler also shares some similarities with mental models theory (MMT) (Johnson-Laird, 1980). Both models posit that the fundamental units of reasoning are concrete possibilities and give special status to certain states (which in MMT are referred to as *initial mental models*). A more recent instantiation of MMT even defines a sampling process in which possibilities (i.e., mental models) are stochastically generated (Johnson-Laird et al., 2015; Khemlani et al., 2014). On this account, reasoners sample (with probability ϵ) from either the set of initial models or the set of

fully explicit models (i.e., all models that are logically consistent with the premises). Model sampling continues until the number of models matches a number drawn from a Poisson distribution. Causal inferences are then drawn on the basis of the sampled models.

Despite these superficial similarities however, the mutation sampler and MMT differ in a number of important ways. One is that they posit different initial states.¹³ A more fundamental difference is that states in MMT are qualitative possibilities consistent with the causal claims and as such do not have probabilities associated with them. Although probabilities can be derived from the sampled models (see Johnson-Laird et al., 2015), the manner in which those probabilities are computed treats the possibilities as equiprobable. For example, for the causal claim “insulting Adam causes Bethany to be angry”, MMT stipulates that the fully explicit models are

- Adam was insulted and Bethany was angry
- Adam was not insulted and Bethany was angry
- Adam was not insulted and Bethany was not angry

This set of models implies that Bethany is angry two-thirds of the time, that the chance that Bethany is angry conditioned on Adam not being insulted is one half, and so forth. In contrast, we believe that when making such judgments human reasoners naturally take into account, for example, their beliefs about how often Bethany tends to be angry and the strength of the causal linkage between the insulting of Adam and Bethany’s resulting anger. This intuition is reflected by the mutation sampler’s fundamentally probabilistic representations that reflect variables’ base rates, the strengths of the causal relations, and so forth. These factors influence causal judgments via the computation of the relative probability of states that occurs during the computation of Metropolis-Hastings transition probabilities.

These differences result in the models making different predictions for a number of key causal judgments. For one, MMT agrees with the normative model, and disagrees with the mutation sampler, by positing the absence of screening off errors in a common cause structure. As demonstrated earlier, there is overwhelming evidence that people do in fact exhibit Markov violations in common cause networks. According to Ali et al. (2011), MMT predicts no explaining away, a foundational signature of causal reasoning (Rottman and Hastie, 2014).¹⁴ In contrast, the mutation sampler can predict explaining away judgments, although weaker than those stipulated by the normative model. Another important difference between models of course is that the mutation sampler but not MMT is an example of a rational process that approximates the normative standard to the extent that sufficient cognitive resources are available.

¹³The initial states specified by the mutation sampler – the prototype states in which variables are either all present or all absent – do not generally correspond to either the initial or fully explicit mental models specified by MMT. For example, for the common cause network $Y_A \leftarrow X \rightarrow Y_B$ the initial models are $\{y_A^1 x^1 y_B^1\}$, that is, the single state in which all variables are present. The set of fully explicit models is formed by adding the logically possible states in which X is absent, resulting in $\{y_A^1 x^1 y_B^1, y_A^0 x^0 y_B^0, y_A^0 x^0 y_B^1, y_A^1 x^0 y_B^1\}$. For the common effect network $Y_A \rightarrow X \leftarrow Y_B$ the initial models are $\{y_A^1 x^1 y_B^1, y_A^1 x^1, x^1 y_B^1\}$ (in initial models only true states are represented, e.g. in model $y_A^1 x^1$ the state of Y_B is omitted rather than explicitly represented as false). The set of fully explicit models is formed by instantiating omitted states and adding the states in which Y_A and Y_B are absent, resulting in $\{y_A^1 x^1 y_B^1, y_A^1 x^1 y_B^0, y_A^0 x^1 y_B^1, y_A^0 x^0 y_B^0, y_A^0 x^1 y_B^0\}$. See Ali et al. (2011) for additional discussion. Note that the fact that the initial models for common cause and common effect networks differ illustrates MMT’s assumption that even causal reasoners (those that reason on the basis of initial models alone) are sensitive to the direction of the causal links. In contrast, the mutation sampler assumes that initial states are independent of network topology.

¹⁴Although whether MMT predicts explaining away depends on exactly what models are represented. Ali et al.’s (2011) predictions were derived assuming that reasoners’ initial models include a representation of the existence of other models, as denoted by the presence of ellipses alongside the initial models. Ali et al. argue that including those potential additional models in the calculation of conditional probability results in the absence of explaining away. In contrast, Johnson-Laird (personal communication, August, 15, 2018) notes the explaining away is predicted if the initial models are considered in isolation. Note that on the basis of full models, MMT predicts the absence of explaining away.

5.2.4 | Accounts Based on Prior Knowledge

Finally, it is worth noting that there exist alternative types of explanations of some of the causal reasoning errors we focus on here. In particular, it has often been argued that apparent causal reasoning errors arise because subjects were reasoning with knowledge in addition to that assumed by the experimenters. For example, Rehder and Burnett (2005) suggested that independence violations arise when variables are features of categories because people believe that many categories possess underlying causal processes that bring rise to observed features (Medin and Ortony, 1989; Gelman, 2004). When instructed on a common cause structure such as the one in Fig. 4A (i.e., $Y_A \leftarrow X \rightarrow Y_B$), Park and Sloman (2013, 2014) observed that reasoners were less likely to treat the Y s as independent conditioned on X when the $X \rightarrow Y_A$ and $X \rightarrow Y_B$ causal relationships were viewed as sharing underlying mechanism and, moreover, that is, that is normative to do so (because, e.g., the presence of an unobserved factor that disables both $X \rightarrow Y_A$ and $X \rightarrow Y_B$ renders the Y s dependent conditioned on X ; also see Hausman & Woodward, 1999; Mayrhofer & Waldmann, 2015; Rehder, 2014; Walsh & Sloman, 2004). For a common effect structure such as the one in Fig. 4B (i.e., $Y_A \rightarrow X \leftarrow Y_B$), explaining away is predicted if reasoners interpret $Y_A \rightarrow X$ and $Y_B \rightarrow X$ as operating independently and integrate according to a noisy-or but not if they believe Y_A and Y_B bring about X conjunctively instead (Rehder, 2015).

It is also possible that prior knowledge was responsible for the Markov violations in the intervention studies presented earlier. Predictions derived from causal graphical models for interventions rely on Pearl's notion of graph surgery (Pearl, 2000), which assumes *ideal* interventions that remove all correlations between a variable and its causes. In contrast, prior domain knowledge might suggest that interventions are not ideal. For example, inoculating a patient dramatically decreases their probability of getting a disease but does not render it absolutely impossible. Thus, interventions that are viewed as non-ideal may have also contributed to the independence violations in those studies.

What such accounts have in common is that they rationalize causal reasoning errors by noting that they may no longer be errors if the subjects' prior knowledge of the situation, rather than the experimenters', is taken into account. However, whereas reasoners in some past studies may have indeed made use of extra-experimental knowledge, work using more advanced methodologies (e.g., full counterbalancing of materials, use of "blank" materials in which variables were simply referred to as "A," "B," etc.) that control for this possibility has shown that some of these errors persist nonetheless (e.g., Rehder, 2014; Rottman & Hastie, 2016; see Rehder, 2018 for an extensive discussion of the account of causal reasoning errors provided by prior knowledge). Rather than positing alternative interpretations of causal knowledge on a case by case basis (disablers for common cause networks, conjunctive causes for common effect networks, non-ideal interventions, etc.), the mutation sampler provides a parsimonious account of the reasoning errors that arise with both a large number of causal network topologies and several types of causal-based judgments.

5.3 | New Empirical Questions

The primary focus of most studies of causal reasoning, including this one, has been on what causal inferences people draw and, in some instances, whether those inferences should be considered normative. By additionally asking *how* those inferences are drawn, we hope that the mutation sampler will expand the kinds of research questions that are posed and the kind of data that is considered. We now present a number of examples of these.

5.3.1 | Variability in Causal Judgments

One avenue of future research concerns the variability inherent in causal judgments. Although little past research has addressed this question, the recent study by Rottman and Hastie (2016) reported not only the mean responses

to conditional probability queries but also histograms of those responses. For example, Fig. 9A shows the histograms of responses to queries associated with a three variable common cause network like the one in Fig. 4A from their Experiments 1A and 1B.¹⁵ The first two columns are labeled “Markov” because they are queries relevant to evaluating independence violations, namely, $p(y_i^1|x^1y_j^0)$ and $p(y_i^1|x^1y_j^1)$. The third and fourth columns presents what Rottman and Hastie referred to as “middle” inferences (an inference to the “middle” X variable, i.e., $p(x^1|y_A^1y_B^1)$) and “transitive” inferences (i.e., $p(y_i^1|y_j^1)$), respectively. In the figure, participants’ ratings have been scaled into the range 0 to 1. A striking feature of Fig. 9A is the large variability associated with each type of response. For example, the range that encompassed 95% of responses to the straightforward $p(y_i^1|y_j^1)$ query was [.19, .96].

Fig. 9B presents the corresponding histograms generated by the mutation sampler assuming a causal strength of *mean* (.750, .875), a background strength of *mean* (.250, .125), and a chain length of 36. Note that whereas the predictions of the mutation sampler presented earlier in this paper were derived by computing the expected value of a joint distribution for a given chain length (and then the corresponding conditional probabilities), those in Fig. 9B were computed by actually running the sampler 100,000 times. The figure shows that the predictions of the mutation sampler exhibits variability comparable to that of Rottman and Hastie’s participants. It also tends to reproduce an unusual feature of their data, which is the presence of “spikes” in the histograms at .50. Such spikes, which might represent uncertainty in the mind of reasoners when reasoning about network states that have apparent inconsistencies (e.g., in $p(y_i^1|x^1y_j^0)$, the common cause X is present but its effect Y_j is absent) or include variables with unspecified values (e.g., in $p(y_i^1|y_j^1)$ the state of X is unspecified). Interestingly, the mutation sampler predicts 0.50 for conditional probability queries when the networks states that are involved in the calculation have not been visited by the stochastic sampling process and thus are at their initialized value.¹⁶ A question for future research concerns whether Fig. 9A reflects within or between participant variability. Assuming that each conditional probability judgment involves another run of the mutation sampler, it predicts both within and between participant variability.

¹⁵We thank Ben Rottman for providing the data from these studies. Experiments 1A ($N = 102$) and 1B ($N = 110$) were identical except that the strengths of the causal relations between X and the Y s (which were conveyed by participants observing individual cases) were 0.750 and .875, respectively, whereas the strength of alternative causes of the Y s were .250 and .125. We collapse across these similar studies in order to obtain a better estimate of the distribution of participants’ responses (one based on $N = 212$).

¹⁶Recall from Section 2.5 that the number of visits to each network state is initialized to 10^{-10} . Using $p(y_i^1|x^1y_j^0)$ as an example, note that $p(y_i^1|x^1y_j^0) = p(x^1y_i^1y_j^0)/[p(x^1y_i^1y_j^0) + p(x^1y_i^0y_j^0)]$ and that states $x^1y_i^1y_j^0$ and $x^1y_i^0y_j^0$ are each unlikely states (because in both X is present but Y_j is absent) and so may not be sampled. When they aren’t, $p(y_i^1|x^1y_j^0) = 10^{-10}/[10^{-10} + 10^{-10}] = 0.50$.

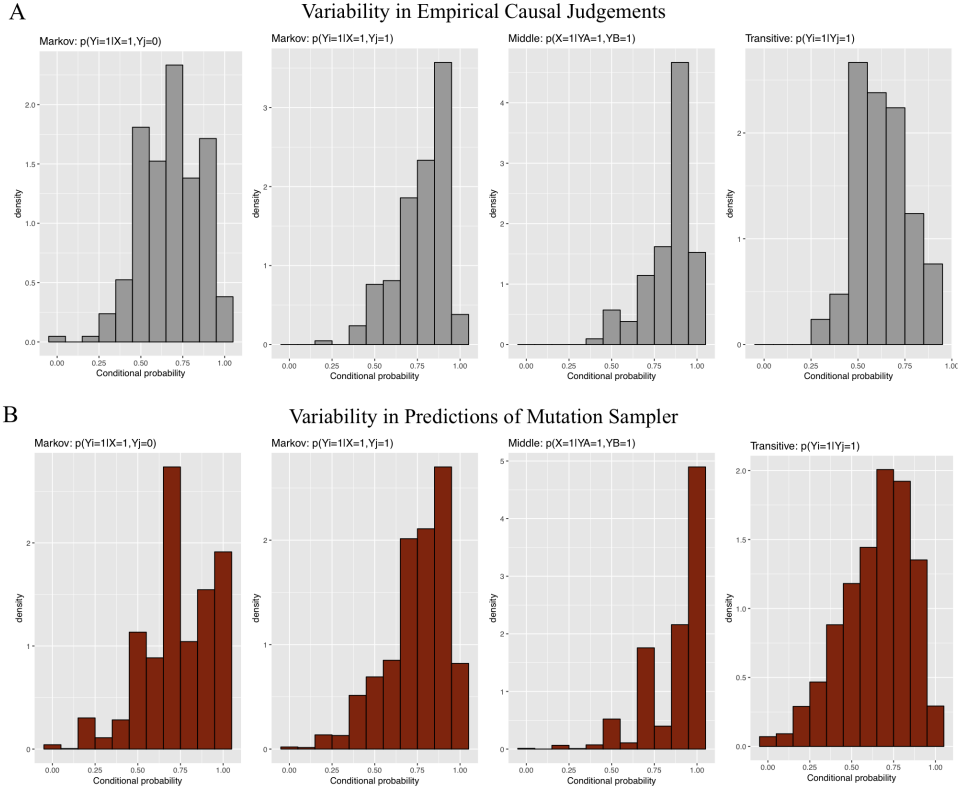


FIGURE 9 (A) Distribution of empirical ratings from Experiments 1A and 1B of Rottman and Hastie (2016). The first two columns present “Markov” inferences ($p(y_i^1|x^1y_j^0)$ and $p(y_i^1|x^0y_j^1)$), the third column presents “middle” inferences ($p(x^1|y_A^1y_B^1)$), and the fourth presents “transitive” inferences ($p(y_i^1|y_j^1)$). The responses have in fact been collapsed over a number of different types of conditional probability queries that were considered equivalent for the purpose of the theoretical questions Rottman and Hastie addressed. For example, the ratings in the first column includes responses to both $p(y_i^1|x^1y_j^0)$ and $p(y_i^1|x^0y_j^1)$, where the latter rating was first flipped around the midpoint of the scale (0.50). Likewise, the second column includes $p(y_i^1|x^1y_j^1)$ and the flipped responses to $p(y_i^1|x^0y_j^0)$, the third includes $p(x^1|y_A^1y_B^1)$ and the flipped responses to $p(x^1|y_A^0y_B^0)$, and the fourth includes $p(y_i^1|y_j^1)$ and the flipped responses to $p(y_i^1|y_j^0)$. (B) The corresponding distributions generated by the mutation sampler.

5.3.2 | Individual Differences

There is also evidence for the presence of systematic differences in how individuals draw causal inferences. For example, Rehder (2014) found that the causal inferences of a substantial minority of subjects exhibited no sensitivity to causal direction (treating, for example, common cause and common effect networks equivalently). These subjects, who Rehder dubbed *associative reasoners*, committed a large number of Markov violations.

Trueblood et al. (2017) also found differences in the magnitude of Markov violations and, moreover, that those violations correlated with other measures, such as the magnitude of order effects (i.e., the difference between $p(Z|X \text{ then } Y)$

and $p(Z|Y \text{ then } X)$) and measures they referred to as *reciprocity* and *memorylessness*. These measures in turn correlated with subjects' performance on the Cognitive Reflection Test (CRT), which is purported to measure differences in reasoners' tendency to emit intuitive versus deliberative responses (Frederick, 2005). That low CRT subjects committed more causal reasoning errors was interpreted by Trueblood et al. as reflecting their tendency to adopt quantum probability representations with low dimensionality, which in fact tend to generate Markov violations, order effects, reciprocity, and memorylessness.

In the context of the mutation sampler, an obvious prediction is that individuals with a larger working memory capacity (and thus a better capacity to generate and maintain long sample chains) might exhibit fewer causal reasoning errors. Indeed, it has been shown that larger working memory capacity correlates with "analytical" thinking more generally (Evans & Over, 2013; Feeney, 2007; Stanovich & West, 1998; Stanovich, 1999). The fact that Markov violations correlate with the CRT (Trueblood et al., 2017), which in turn correlates with measures of general intelligence (Frederick, 2005; Toplak et al., 2011), lends credence to this possibility. A related prediction would be larger causal reasoning errors for participants under working memory load.

5.3.3 | Reaction Times

Although reaction times have received relatively little attention in the causal reasoning literature, time pressure has been shown to increase people's tendency to emit intuitive versus deliberate responses in reasoning more generally (e.g., Evans & Curtis-Holmes, 2005; Evans et al., 2009; Finucane et al., 2000; Roberts & Newton, 2001). A prediction readily derivable from the mutation sampler is that time pressure will limit the number of samples and thus the accuracy of the inferences drawn. One study that addressed this question in a preliminary way is that of (Rehder, 2014), who manipulated whether or not subjects were given a deadline to respond. In fact, Rehder found no impact of response deadlines on the magnitude of Markov violations. For a number of reasons however, this question deserves additional study. For one, the task in (Rehder, 2014) was a relatively complex one in which subjects had to choose which of two scenarios was more likely to display a particular variable and this need to compare may have affected the mental processes invoked. It is also possible that the deadline used was not sufficient to induce the pressure needed to affect the subjects' sampling process.

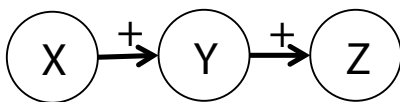
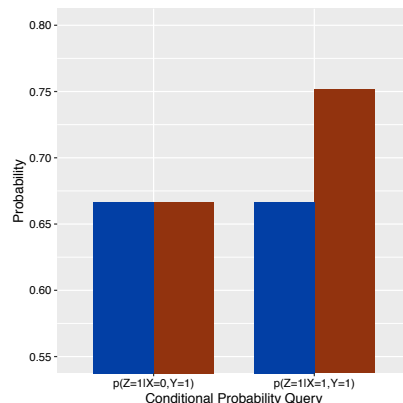
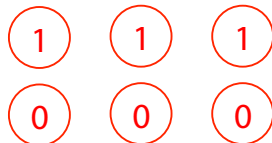
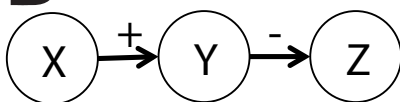
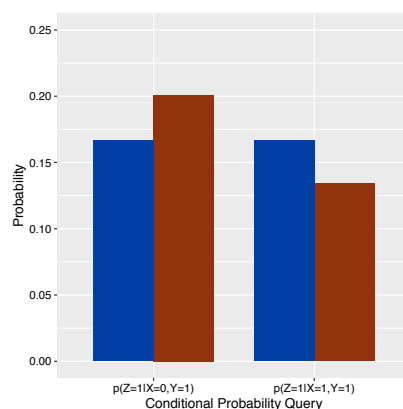
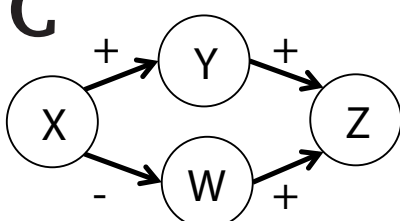
5.3.4 | Generalizing to Additional Causal Scenarios

One strength of the current work is that it has tested the mutation sampler on a relatively large number of judgment types and causal network topologies. Yet, one limitation of those tests is that the causal networks only involved generative causal relations. This limitation allowed us to present a simplified view of prototypes states. Recall that we justified prototypes as plausible states at which to commence sampling because they are easily identifiable as consistent with the causal relations on the basis of a qualitative analysis of the causal network, namely, one that ignores the strength, direction, and functional form of the causal relations. Applying that justification to networks with only generative relations yields prototype states in which binary variables are all present or all absent, an assumption made in all the model fitting reported above. However, applying the justification to networks that also include *inhibitory* causal relations may yield different prototypes. For example, compare the two three-variable chain networks in panels A and B of Fig. 10. The chain in panel A has generative causal relations and so the usual prototypes (variables all present or all absent). For this network, the chart in Fig. 10A shows that the mutation sampler yields a Markov violation in the usual direction: the probability of $Z = 1$ conditioned on $Y = 1$ is greater when X is also present as compared to when it is absent. (The predictions of the normative model, also shown in the chart, of course reflect independence:

$p(z^1|x^0y^1) = p(z^1|x^1y^1)$.) In comparison, in panel B the causal relation between $Y \rightarrow Z$ is *inhibitory* rather than generative. For this network, our recipe for identifying prototypes—identify states that are qualitatively consistent with the causal relations—yields $x^1y^1z^0$ and $x^0y^0z^1$, that is, states in which Y and Z have opposite values, befitting the inhibitory relation between them. Importantly, although these prototypes also yield Markov violations the direction of those violations might change. The chart in Fig. 10B shows that a mutation sampler supplied with prototypes $x^1y^1z^0$ and $x^0y^0z^1$ predicts that $p(z^1|x^1y^1)$ will be *less than* instead of greater than $p(z^1|x^0y^1)$.

Mixtures of generative and inhibitory relations can yield cases in which no prototypes are identifiable. Consider the network in Fig. 10C. The $X \rightarrow Y \rightarrow Z$ subnetwork implies that X and Z should have the same values in a potential prototype whereas the $X \rightarrow W \rightarrow Z$ subnetwork implies they should have opposite values. Thus, there are no prototype states that are qualitatively consistent with this network's causal relations. In fact, the chart in Fig. 10C shows that a mutation sampler that starts sampling at a randomly chosen system state (a.k.a., the unbiased sampler) yields the virtual absence of an independence violation ($p(z^1|x^0y^1) \approx p(z^1|x^1y^1)$). The novel predictions shown in Fig. 10 are readily testable with additional empirical work.

The mutation sampler could also be applied to networks with continuous variables. Although most studies test binary variables, Rottman and Hastie (2016) found that the same pattern of independence violations obtains with continuous variables (e.g., in a $Y_A \leftarrow X \rightarrow Y_B$ common cause network, a larger value of Y_A led to a larger estimate of Y_B even when the state of X was known). Application of the mutation sampler to such cases would involve shifting probability mass in the joint probability density function; application of the sampling model would involve starting MCMC sampling at states in which X , Y_A , and Y_B all have either high values or low ones.

APrototypes**B**Prototypes**C**Prototypes

???

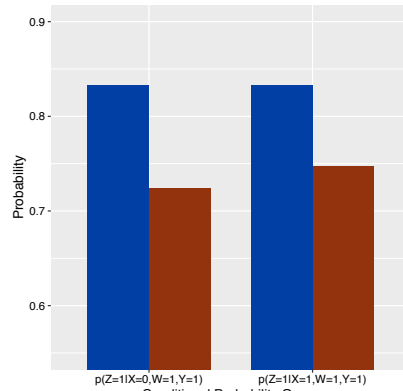


FIGURE 10 Visualization of different prototype states depending on causal structure, and resulting conditional probability judgments for the normative model (blue) and mutation sampler (red) given those prototypes. For both models, the marginal probability of the causes = .50, the strength of background causes = .33, and the causal strength = .50 (where for inhibitory causal relations, causal strength refers to the probability of the cause preventing the effect from occurring). Judgments for the mutation sampler were the expected values after 8 samples.

5.3.5 | Empirical Learning of Causal Relations

Finally, many of the fits of mutation sampler presented in this article were to studies that simply instructed subjects on the existence of causal relations without also presenting learning data that exemplified those relations. This raises the question of how the sampling approach applies when such data is present. On one hand, studies that have presented learning data have found that they are not sufficient to eliminate the errors we've considered here (e.g., Markov violations, Rehder & Davis, 2016, Rehder & Waldmann, 2017; Rottman & Hastie, 2016, and Waldmann & Hagnayer, 2005). On the other, Rehder and Waldmann (2017) systematically manipulated the presence/non-presence of learning data and found that those errors were reduced in magnitude and, moreover, disappeared entirely when subjects were provided with data but not a verbal description of the causal relations. Overall, these results are consistent with our conjecture that prototypes, because they are easily ascertained to be consistent with (a verbal description of) the causal relations, naturally come to reasoners' mind and so are likely to serve as a point to start a sampling chain. But if learning data is also available then a previously observed system state could serve as the starting point instead, ameliorating or eliminating the reasoning biases induced by the prototypes. In fact, there is evidence that people do just such a thing in some circumstances (Dasgupta et al., 2018). Future experiments could test the possibility that sampling commences at a previously observed system state by, for example, manipulating the probability that that state was brought to mind just before a causal inference. This approach would be analogous to manipulating the anchor in a traditional anchoring and adjustment experiment (Lieder et al., 2012; Tversky and Kahneman, 1974). The mutation sampler could readily be used to predict subjects' most likely causal inference as a function of which system state the sampling chain was "anchored" on.

5.4 | Conclusion

The successes of the mutation sampler demonstrate that it can account for people's generally good causal reasoning performance while also explaining the systematic errors they make. Nevertheless, as a rational process model, the mutation sampler embodies the view that humans *could* draw veridical causal inferences — if only they had the cognitive resources to do so. The fault lies in the fact that causal judgments must be computed in finite time and with limited resources. Errors in causal reasoning are thus an unavoidable consequence of the tradeoff between accuracy, speed, and effort.

Although the causal graphical model framework has served as a useful characterization of causal cognition, less work has investigated how such inferences can be drawn in a psychologically plausible manner. We have proposed that causal judgments are based on a relatively small number of samples drawn from a causal system and applied that approach to a large number of causal-based tasks, experimental conditions, and participants. We claim that the mutation sampler strikes an appropriate balance between the fact that people largely succeed at making sophisticated causal judgments while also committing systematic errors. And we have argued that the computations and representations required by mutation sampling are within the reach of most reasoners for most types of judgments. We hope that the development of causal process models will expand the kinds of phenomena typically considered in the causal cognition literature, including the variability of causal judgments, inter-individual differences in reasoning strategies, and reaction times.

references

- Ali, N., Chater, N. and Oaksford, M. (2011) The mental representation of causal conditional reasoning: Mental models or causal models. *Cognition*, **119**, 403–418.

- Anderson, J. R. (1990) *The adaptive character of thought*. Psychology Press.
- Bramley, N. R., Dayan, P., Griffiths, T. L. and Lagnado, D. A. (2017) Formalizing neurath's ship: Approximate algorithms for online causal learning. *Psychological review*, **124**, 301.
- Burnham, K. P. and Anderson, D. R. (1998) Model selection and inference: a practical information-theoretical approach. New-York: Springer-Verlag.
- Casella, G. and George, E. I. (1992) Explaining the gibbs sampler. *The American Statistician*, **46**, 167–174.
- Cheng, P. W. (1997) From covariation to causation: a causal power theory. *Psychological review*, **104**, 367.
- Dasgupta, I., Schulz, E. and Gershman, S. J. (2017) Where do hypotheses come from? *Cognitive psychology*, **96**, 1–25.
- Dasgupta, I., Schulz, E., Goodman, N. D. and Gershman, S. J. (2018) Remembrance of inferences past: Amortization in human hypothesis generation. *Cognition*, **178**, 67–81.
- Evans, J. S. B. and Curtis-Holmes, J. (2005) Rapid responding increases belief bias: Evidence for the dual-process theory of reasoning. *Thinking & Reasoning*, **11**, 382–389.
- Evans, J. S. B., Handley, S. J. and Bacon, A. M. (2009) Reasoning under time pressure: A study of causal conditional inference. *Experimental Psychology*, **56**, 77–83.
- Evans, J. S. B. and Over, D. E. (2013) *Rationality and reasoning*. Psychology Press.
- Feeney, A. (2007) Individual differences, dual processes, and induction. *Inductive reasoning*, 302–327.
- Fernbach, P. M. and Rehder, B. (2013) Cognitive shortcuts in causal inference. *Argument & Computation*, **4**, 64–88.
- Finucane, M. L., Alhakami, A., Slovic, P. and Johnson, S. M. (2000) The affect heuristic in judgments of risks and benefits. *Journal of behavioral decision making*, **13**, 1–17.
- Frederick, S. (2005) Cognitive reflection and decision making. *Journal of Economic perspectives*, **19**, 25–42.
- Gelman, S. A. (2004) Psychological essentialism in children. *Trends in cognitive sciences*, **8**, 404–409.
- Griffiths, T. L., Chater, N., Kemp, C., Perfors, A. and Tenenbaum, J. B. (2010) Probabilistic models of cognition: Exploring representations and inductive biases. *Trends in cognitive sciences*, **14**, 357–364.
- Griffiths, T. L., Lieder, F. and Goodman, N. D. (2015) Rational use of cognitive resources: Levels of analysis between the computational and the algorithmic. *Topics in cognitive science*, **7**, 217–229.
- Griffiths, T. L. and Tenenbaum, J. B. (2005) Structure and strength in causal induction. *Cognitive psychology*, **51**, 334–384.
- Hagmayer, Y. (2016) Causal bayes nets as psychological theories of causal reasoning: evidence from psychological research. *Synthese*, **193**, 1107–1126.
- Hastings, W. K. (1970) Monte carlo sampling methods using markov chains and their applications. *Biometrika*, **57**, 97–109.
- Hausman, D. M. and Woodward, J. (1999) Independence, invariance and the causal markov condition. *The British journal for the philosophy of science*, **50**, 521–583.
- Hertwig, R. and Pleskac, T. J. (2010) Decisions from experience: Why small samples? *Cognition*, **115**, 225–237.
- Johnson, J. G. and Busemeyer, J. R. (2016) A computational model of the attention process in risky choice. *Decision*, **3**, 254.
- Johnson-Laird, P. N. (1980) Mental models in cognitive science. *Cognitive science*, **4**, 71–115.

- Johnson-Laird, P. N., Khemlani, S. S. and Goodwin, G. P. (2015) Logic, probability, and human reasoning. *Trends in cognitive sciences*, **19**, 201–214.
- Khemlani, S. S., Barbey, A. K. and Johnson-Laird, P. N. (2014) Causal reasoning with mental models. *Frontiers in human neuroscience*, **8**, 849.
- Koehler, D. J. (1994) Hypothesis generation and confidence in judgment. *Journal of Experimental Psychology: Learning, Memory, and Cognition*, **20**, 461.
- Koller, D. and Friedman, N. (2009) *Probabilistic graphical models: principles and techniques*. MIT press.
- Lagnado, D. A. and Sloman, S. (2004) The advantage of timely intervention. *Journal of Experimental Psychology: Learning, Memory, and Cognition*, **30**, 856.
- Lieder, F., Griffiths, T. and Goodman, N. (2012) Burn-in, bias, and the rationality of anchoring. In *Advances in neural information processing systems*, 2690–2798.
- Luhmann, C. C. and Ahn, W.-k. (2007) Buckle: A model of unobserved cause learning. *Psychological review*, **114**, 657.
- Marr, D. (1982) *Vision: A Computational Investigation into the Human Representation and Processing of Visual Information*. New York, NY, USA: Henry Holt and Co., Inc.
- Mayrhofer, R. and Waldmann, M. R. (2015) Agents and causes: Dispositional intuitions as a guide to causal structure. *Cognitive science*, **39** 1, 65–95.
- Medin, D. and Ortony, A. (1989) Psychological essentialism. In *Similarity and analogical reasoning* (ed. A. Ortony). Cambridge University Press.
- Morris, M. W. and Larrick, R. P. (1995) When one cause casts doubt on another: A normative analysis of discounting in causal attribution. *Psychological Review*, **102**, 331.
- Park, J. and Sloman, S. A. (2013) Mechanistic beliefs determine adherence to the markov property in causal reasoning. *Cognitive Psychology*, **67**, 186–216.
- (2014) Causal explanation in the face of contradiction. *Memory & cognition*, **42**, 806–820.
- Pearl, J. (1988) *Probabilistic reasoning in intelligent systems: networks of plausible inference*. Elsevier.
- (2000) *Causality: models, reasoning and inference*, vol. 29. Springer.
- Perales, J. C., Catena, A. and Maldonado, A. (2004) Inferring non-observed correlations from causal scenarios: The role of causal knowledge. *Learning and Motivation*, **35**, 115–135.
- Rehder, B. (2003a) Categorization as causal reasoning. *Cognitive Science*, **27**, 709–748.
- (2003b) A causal-model theory of conceptual representation and categorization. *Journal of Experimental Psychology: Learning, Memory, and Cognition*, **29**, 1141.
- (2014) Independence and dependence in human causal reasoning. *Cognitive psychology*, **72**, 54–107.
- (2015) The role of functional form in causal-based categorization. *Journal of Experimental Psychology: Learning, Memory, and Cognition*, **41**, 670.
- (2018) Beyond markov: Accounting for independence violations in causal reasoning. *Cognitive psychology*, **103**, 42–84.
- Rehder, B. and Burnett, R. C. (2005) Feature inference and the causal structure of categories. *Cognitive Psychology*, **50**, 264–314.

- Rehder, B. and Davis, Z. (2016) Evaluating causal hypotheses: the curious case of correlated cues. In *CogSci*, vol. 38. Cognitive Science Society.
- Rehder, B. and Hastie, R. (2001) Causal knowledge and categories: The effects of causal beliefs on categorization, induction, and similarity. *Journal of Experimental Psychology: General*, **130**, 323.
- Rehder, B. and Kim, S. (2006) How causal knowledge affects classification: A generative theory of categorization. *Journal of Experimental Psychology: Learning, Memory, and Cognition*, **32**, 659.
- (2008) The role of coherence in causal-based categorization. In *Proceedings of the Annual Meeting of the Cognitive Science Society*, vol. 30.
- (2010) Causal status and coherence in causal-based categorization. *Journal of Experimental Psychology: Learning, Memory, and Cognition*, **36**, 1171.
- Rehder, B. and Waldmann, M. R. (2017) Failures of explaining away and screening off in described versus experienced causal learning scenarios. *Memory & cognition*, **45**, 245–260.
- Roberts, M. J. and Newton, E. J. (2001) Inspection times, the change task, and the rapid-response selection task. *The Quarterly Journal of Experimental Psychology: Section A*, **54**, 1031–1048.
- Rottman, B. M. and Hastie, R. (2014) Reasoning about causal relationships: Inferences on causal networks. *Psychological bulletin*, **140**, 109.
- (2016) Do people reason rationally about causally related events? markov violations, weak inferences, and failures of explaining away. *Cognitive Psychology*, **87**, 88–134.
- Stanovich, K. E. (1999) *Who is rational?: Studies of individual differences in reasoning*. Psychology Press.
- Stanovich, K. E. and West, R. F. (1998) Individual differences in rational thought. *Journal of experimental psychology: general*, **127**, 161.
- Toplak, M. E., West, R. F. and Stanovich, K. E. (2011) The cognitive reflection test as a predictor of performance on heuristics-and-biases tasks. *Memory & cognition*, **39**, 1275.
- Trueblood, J. S. and Busemeyer, J. R. (2012) A quantum probability model of causal reasoning. *Frontiers in Psychology*, **3**, 138.
- Trueblood, J. S., Yearsley, J. M. and Pothos, E. M. (2017) A quantum probability framework for human probabilistic inference. *Journal of Experimental Psychology: General*, **146**, 1307.
- Tversky, A. and Kahneman, D. (1974) Judgment under uncertainty: Heuristics and biases. *science*, **185**, 1124–1131.
- Van Ravenzwaaij, D., Cassey, P. and Brown, S. D. (2018) A simple introduction to markov chain monte-carlo sampling. *Psychonomic bulletin & review*, **25**, 143–154.
- Von Sydow, M., Hagnayer, Y., Meder, B. and Waldman, M. R. (2010) How causal reasoning can bias empirical evidence. In *Proceedings of the Annual Meeting of the Cognitive Science Society*, vol. 32.
- Vul, E., Goodman, N., Griffiths, T. L. and Tenenbaum, J. B. (2014) One and done? optimal decisions from very few samples. *Cognitive science*, **38**, 599–637.
- Vul, E. and Pashler, H. (2008) Measuring the crowd within: Probabilistic representations within individuals. *Psychological Science*, **19**, 645–647.
- Waldmann, M. R. and Hagnayer, Y. (2005) Seeing versus doing: two modes of accessing causal knowledge. *Journal of Experimental Psychology: Learning, Memory, and Cognition*, **31**, 216.
- (2013) Causal reasoning.
- Walsh, C. R. and Sloman, S. A. (2004) Revising causal beliefs. In *Proceedings of the Annual Meeting of the Cognitive Science Society*, vol. 26.

TABLE 3 Example Conditional Probability Distributions for the network in Fig. 2.

Mutated variable	State of parent variables	Conditional probability expression	Conditional probability
a^1		c_A	.600
b^1		c_B	.600
c^1	$a^1 b^1$	$1 - (1 - b_C)(1 - m_{AC})(1 - m_{BC})$.911
	$a^0 b^1$	$1 - (1 - b_C)(1 - m_{BC})$.733
	$a^1 b^0$	$1 - (1 - b_C)(1 - m_{AC})$.733
	$a^0 b^0$	b_C	.200
d^1	b^1	$1 - (1 - b_D)(1 - m_{BC})$.733
	b^0	b_D	.200
e^1	c^1	$1 - (1 - b_E)(1 - m_{CE})$.733
	c^0	b_E	.200

6 | APPENDIX A: COMPUTING METROPOLIS-HASTINGS TRANSITION PROBABILITIES

We present quantitative examples of Metropolis-Hastings ratios for the network in Fig. 2. Doing so requires assumptions regarding the functions that link causes to their effects. One possibility, which corresponds to the conditions in the large majority of empirical studies that are considered later in this article, are that the causal links are *generative* (a cause makes its effects more likely) and *independent* (each causal link operates autonomously) and that multiple causal influences integrate according to a *noisy-or* function (Cheng, 1997). The generating function that defines the probability of variable V_i being present is then

$$\pi(v_i^1 | Pa(V_i)) = 1 - (1 - b_i) \sum_{V_j \in Pa(V_i)} (1 - m_{ji})^{ind(V_j)}$$

where $Pa(V_i)$ denotes the parents of V_i , m_{ji} is the strength of the causal link between parent variable V_j and V_i , $ind(V_j)$ is an indicator function that yields 1 if V_j is present and 0 otherwise, and b_i is the effect of background causes on V_i (causal influences exogenous to the model). If variable V_i is a “root” variable (i.e., has no causal parents), the probability that it is present is given by parameter c_{V_i} . Note that the principle of *causal sufficiency* that accompanies causal graphical models – that graph variables have no hidden causes in common – entails that root nodes are independent of one another.

Table 3 presents the probabilities of each variable in Fig. 2 as a function of the state of its parents assuming that the marginal probabilities of the root causes A and B (c_A and c_B) are .60, that all causal relations (m_{AC} , m_{BC} , m_{BD} , and m_{AC}) have a strength of .67, and that the strength of the background causes for the remaining variables (b_C , b_D , and b_E) is .20. The probabilities in Table 3 constitute what is referred to as the *conditional probability distributions* (CPDs) for the network in Fig. 2 under the given parameterization.

CPDs may be derived from generating functions other than a noisy-or of course. For example, rather than serving as independent causes of C in Fig. 2, A and B might be *conjunctive causes* such that both need to be present in order to generate C .

$$\pi(c^1 | ab) = 1 - (1 - b_C)(1 - m_{ABC})^{ind(A)ind(B)}$$

where m_{ABC} is the strength of the conjunctive causal relationship relating A , B , and C . One empirical study considered in Appendix C instructed subjects on conjunctive causal relationships.

A causal graph's CPDs are sufficient to compute any marginal, conditional, and joint probability associated with that graph. For example, the Markov condition associated with causal graphical models stipulates that the graph in Fig. 2 factors such that $p(abce) = p(e|c)p(d|b)p(c|ab)p(a)p(b)$. Of course, any marginal and conditional probability can be derived from the joint.

We now show how a causal graph's CPDs are also sufficient to efficiently compute Metropolis-Hastings (MH) transition probabilities. Consider the first example MH ratio in Fig. 2, $\pi(c'e')/\pi(c'e)$. Suppose that c^1e^0 holds in the current state q and the value of E has mutated to 1 in the proposed state q' . Noting that $\pi(c'e) = \pi(e|c)\pi(c)$, the MH ratio can be computed from the CPDs in Table 3.

$$\frac{\pi(c^1e^1)}{\pi(c^1e^0)} = \frac{\pi(e^1|c^1)\pi(c^1)}{\pi(e^0|c^1)\pi(c^1)} = \frac{\pi(e^1|c^1)}{\pi(e^0|c^1)} = \frac{.733}{1 - .733} = 2.75$$

Table 4 presents the MH ratios for the cases in which E mutates to 1 as a function of the two possible values of C (c^0 and c^1).

The second example MH ratio in Fig. 2 is $\pi(a'b'c)/\pi(abc)$. Suppose that $a^0b^1c^0$ holds in the current state q and the value of A has mutated to 1 in the proposed state q' . Noting that $\pi(abc) = \pi(c|ab)\pi(a)\pi(b)$ and substituting in the appropriate CPDs from Table 3,

$$\frac{\pi(a^1b^1c^0)}{\pi(a^0b^1c^0)} = \frac{\pi(c^0|a^1b^1)\pi(a^1)\pi(b^1)}{\pi(c^0|a^0b^1)\pi(a^0)\pi(b^1)} = \frac{\pi(c^0|a^1b^1)\pi(a^1)}{\pi(c^0|a^0b^1)\pi(a^0)} = \frac{(1 - .911)(.60)}{(1 - .733)(1 - .60)} = 0.500$$

Table 4 presents the MH ratios for the case in which A mutates to 1 as a function of the four possible values of B and C .

The third example MH ratio in Fig. 2 is $\pi(abc'e)/\pi(abce)$. Suppose that $a^0b^1c^0e^0$ holds in the current state q and the value of C has mutated to 1 in the proposed state q' . Noting that $\pi(abce) = \pi(e|c)\pi(c|ab)\pi(a)\pi(b)$ and substituting in the appropriate CPDs from Table 3,

$$\frac{\pi(a^0b^1c^1e^0)}{\pi(a^0b^1c^0e^0)} = \frac{\pi(e^0|c^1)\pi(c^1|a^0b^1)\pi(a^0)\pi(b^1)}{\pi(e^0|c^0)\pi(c^0|a^0b^1)\pi(a^0)\pi(b^1)} = \frac{\pi(e^0|c^1)\pi(c^1|a^0b^1)}{\pi(e^0|c^0)\pi(c^0|a^0b^1)} = \frac{(1 - .733)(.733)}{(1 - .20)(1 - .733)} = 0.917$$

Table 4 presents the MH ratios for the case in which C mutates to 1 as a function of the eight possible values of A , B , and E .

These examples illustrate how MH transition probabilities can be computed from a graph's CPDs. Notably, they can be computed without the full joint probability distribution.

7 | APPENDIX B: CONVERGENCE PROPERTIES

This appendix justifies prototype states as a reasonable starting point given initial uncertainty about which states are highly probable for any particular graph. One consequence of generative causal relationships is that they yield positive correlations between variables. Thus, a reasonable first approximation of a graph's joint distribution is one in which

TABLE 4 Examples of Metropolis-Hastings Ratios.

	State of Markov blanket	MH Ratio
$\pi(c\epsilon^1)/\pi(c\epsilon^0)$	c^1	2.75
	c^0	0.25
$\pi(a^1bc)/\pi(a^0bc)$	b^1c^1	1.86
	b^0c^1	5.50
	b^1c^0	0.50
	b^0c^0	0.50
$\pi(ac^1be)/\pi(ac^0be)$	$a^1b^1e^1$	37.58
	$a^1b^1e^0$	3.42
	$a^1b^0e^1$	10.08
	$a^0b^1e^1$	10.08
	$a^1b^0e^0$	0.92
	$a^0b^1e^0$	0.92
	$a^0b^0e^1$	0.92
	$a^0b^0e^0$	0.08

graph states are more probable to the extent they exhibit *coherence*, variables that exhibit the same value. According to this approximation, prototype states are maximally coherent and thus serve as the best states at which to commence sampling. In fact, we show that this strategy often results in faster convergence to the normative distribution as compared to unbiased (uniformly randomly chosen) starting points. Of course, because cognitive resource limitations preclude large number of samples, this result implies that biasing the starting point results in more accurate causal inferences on average. Therefore, although the term “bias” may imply a maladaptive process, in fact it is consistent with our claim that people are capable causal reasoners that commit small but systematic errors.

We randomly generated 360,000 directed acyclic graphs of five binary variables. The graphs were generated by varying two factors—the strength and density of the causal relations—over 30 evenly spaced values from 0 to 1. A density value determined the number of causal links that were randomly chosen from the 10 causal links that define a five-variable network that is fully connected and includes no cycles. For example, the graph in Fig. 2 has four causal relations and thus has a density of .40. Each cell in the 30 x 30 grid was sampled 400 times. In each graph, the marginal probability of a root cause (a variable that has no parent) was set to 0.5 and the strength of alternative causes for each non-root variable was set to 0.1. Together these factors define a normative joint distribution over the five variables for each of the 360,000 graphs.

For each graph, two variants of the mutation sampler (biased or unbiased initialization) were then run with a chain length of exactly eight. For each of these (sampled) distributions, the KL divergence between it and the normative distribution was computed. Fig. 11 shows the square rooted difference in KL-divergence between the biased and unbiased initialization for each parameter combination.¹⁷ Approximately 55% of the 360,000 runs resulted in faster convergence (i.e. lower KL-divergence) for the biased initialization.

The figure shows that biased initialization converged faster in dense graphs with strong causal links, because in such graphs the two prototypes will in fact be highly probable. In contrast, unbiased initialization converged faster in sparse graphs with strong causal links because the sparsity of the causal links means that maximally coherent items need not be the most probable. This result suggests that a biased initialization can be an effective approach given

¹⁷We take the square root for visualization purposes only.

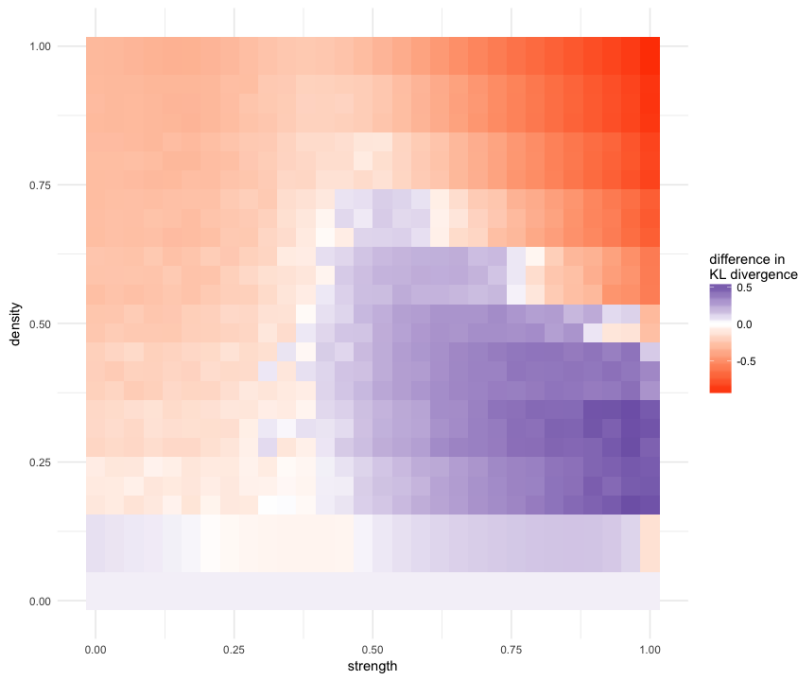


FIGURE 11 Heatmap of $\sqrt{D_{KL}(P||Q_{bias}) - D_{KL}(P||Q_{unbias})}$, where Q_{bias} refers to the estimated joint for a biased initialization. Red squares correspond to a benefit for biased initialization, and blue squares correspond to a benefit for unbiased initialization. Saturation corresponds to the magnitude of difference in KL divergence (larger differences have higher saturation).

initial uncertainty about which graph states are most probable.

8 | APPENDIX C: MODEL FITS TO CONDITIONAL REASONING STUDIES

The normative model and mutation sampler were fit to causal reasoning data from 18 experimental conditions reported in four articles. Each of those conditions is described briefly in Table 4 and in greater detail below.

Rehder and Burnett (2005) (referred to as RB05 in Table 5) taught participants categories whose features were causally related and then asked them to judge the probability that a category member had a feature given a number of the category member's features. In every experiment categories had four features. Experiment 1 tested a common cause network (hereafter referred to as CC network) in which a single feature caused three others. Conditional probability queries presented a category member in which the state of three features was given and asked participant to predict a third feature. Experiment 2 was identical to Experiment 1 except that "blank" materials were used, that is, the domain of the category was not identified and the features were simply referred to as "A," "B," etc. Experiment 3 was identical to Experiment 1 except that there were two rather than three "given" features in the conditional probability queries. Experiment 4 was identical to Experiment 3 except that the four features formed a common effect network a single feature was caused by three others. The three features were described as independent causes of the effect (thus, a CE-Indep. network). In Experiment 5 the features formed a causal chain (CH) and there were three given features in the conditional probability queries.

Rehder (2015) (R15 in Table 5) also tested causally-related category features. All categories had six features. In Experiment 1, three features formed a common effect network in which two features independently caused a third (CE-Indep.). The other three features formed a common effect network in which two features conjunctively caused a third (CE-Conj.). Experiment 2 tested two between-participant conditions. In one, the two triplets of features each formed an independent common effect network but in one triplet the causal relations were described as only operating "occasionally" (CE-Indep. [weak]) whereas in the other they were described as operating "often" (CE-Indep. [strong]). In the other between participant condition the triplets each formed a conjunctive common effect network and the links were either weak (CE-Conj. [weak]) or strong (CE-Conj. [strong]).

Rehder and Waldmann (2017) (RW17) instructed participants on two causal relationships taken from the domain of either economics, sociology, or meteorology. Those relationships formed a common effect network in Experiment 1 and a common cause network in Experiment 2. Each experiment compared between-participant conditions in which participants were given either just a causal network, just data generated from that causal network, or both; here we present fits to the conditions in which participants were only given a causal network.

Using the same materials as Rehder and Waldmann (2017), Rehder (2018) (R18) conducted three experiments that each tested an extended common cause network (in which the effects themselves had effects: $Z_A \leftarrow Y_A \leftarrow X \rightarrow Y_B \rightarrow Z_B$) and an extended common effect network (in which the causes themselves had causes: $Z_A \rightarrow Y_A \rightarrow X \leftarrow Y_B \leftarrow Z_B$). The number of distinct types of conditional probability judgments was 19 in Experiment 1 and 27 in Experiments 2 and 3. In Experiment 3 only participants were told that the causal relations operated 75% of the time.

In each condition participants' ratings were fit according to

$$\text{rating}(t_i) = s * p_{M,\theta_M}(t_i)$$

where M is a model, θ_M are its parameters, t_i is a test item (i.e., a conditional probability query). Both the normative model and the mutation sampler were used to derive a joint probability distribution via the methods described in Appendix A, which was then used to derive the conditional probability appropriate for each test item. Although in general a causal graph's c parameters (representing the marginal probabilities of the root variables), m parameters (representing the strengths of the causal links), and b parameters (representing the strengths of causes extrinsic to the

graph) can all differ from one another, the materials and counterbalancing used in the above studies were such that these parameters could be collapsed into a single c , a single m , and a single b (which, because they represent probabilities, were each constrained to the range [0, 1]). Parameter s (constrained to the range 0-300) is a scaling parameter that maps M 's predictions onto the 0-100 response scale. The mutation sampler included an additional λ parameter representing the mean chain length, constrained to the range [2, 64]. The models were fit to each participant's causal judgments by identifying parameters that minimized squared error.

For each experimental condition, Table 5 presents the number of variables in the network, the number of participants tested in that condition, and the number of distinct types of conditional probability queries they answered. For both the normative model and the mutation sampler it also presents the model's best fitting parameters averaged over participants and a number of measures of fit, including the correlation between predicted and observed values averaged over participants (R), and a measure (AIC) that takes into account a model's number of parameters¹⁸. Finally, the last column of Table 5 presents the percentage of participants best fit by the mutation sampler in each condition. The table indicates that the mutation sampler yielded a better fit as compared to the normative model in all 19 experimental conditions. In addition, a larger number of participants were better fit by the mutation sampler in 16 of the 19 conditions.

¹⁸AIC = $n \cdot \log(SSE/n) + 2 \cdot (p + 1)$ where SSE = sum of squared error, n = number of data points fit and p = a model's number of parameters. This measure was deemed by Burnham and Anderson (1998) as appropriate for comparing models fit by least squares.

TABLE 5 Fits of the normative model and the mutation sampler to past inference studies. Values in bold italic red reflect cases in which the mutation sampler yielded a better fit as compared to the normative model.

Study	Expt.	Condition	No. of network variables	No. of subjects	No. of judgment types	Model	Parameters					Measures of fit			
							c	m	m_2	b	λ	s	R	AIC	Pct. subjects
RW17	1	CE-I	3	48	11	Norm	.401	.483		.178		158	.880	2981.6	
	2	CC				MS	.446	.467		.256	17.9	128	.910	2933.1	38%
	1	CC	4	24	10	Norm	.536	.666		.335		157	.884	3031.2	
	2	CC				MS	.416	.370		.371	6.2	130	.929	2681.5	69%
RB05	1	CC	4	24	10	Norm	.485	.675		.244		116	.879	1468.4	
	2	CC				MS	.682	.753		.414	6.3	104	.929	1255.3	63%
	3	CC	4	24	10	Norm	.676	.612		.438		111	.693	1605.1	
	4	CE-I				MS	.602	.379		.397	7.8	111	.686	1604.9	54%
	5	Chain	4	18	32	Norm	.553	.658		.257		112	.796	1470.6	
	6	CE-I				MS	.637	.325		.438	3.9	98	.834	1366.7	68%
	7	CE-C	4	24	10	Norm	.396	.427		.040		139	.842	1447.0	
	8	CE-C				MS	.539	.503		.176	6.6	108	.948	1267.1	70%
R15	1	CE-I & CE-C	6	48	14	Norm	.463	.661	.763	.147		134	.882	4220.1	
	2	CE-I (weak) & CE-I (strong)				MS	.523	.712	.839	.201	5.1	105	.938	3848.0	73%
	3	CE-C (weak) & CE-C (strong)	6	48	14	Norm	.549	.569	.712	.150		125	.899	3826.7	
	4	CE-C (weak) & CE-C (strong)				MS	.525	.508	.683	.226	8.4	109	.931	3674.0	52%
R18	1	CC	5	48	19	Norm	.290	.409	.516	.163		196	.868	4078.0	
	2	CE-I				MS	.551	.495	.720	.313	3.5	107	.923	3794.0	73%
	3	CC	5	60	27	Norm	.478	.534		.264		128	.773	5324.7	
	4	CE-I				MS	.465	.294		.378	11.1	115	.864	4904.8	81%
	5	CC	5	60	27	Norm	.488	.549		.219		140	.765	5144.6	
	6	CE-I				MS	.464	.396		.256	26.5	117	.799	5056.0	52%
	7	CC	5	60	27	Norm	.461	.547		.239		136	.781	9495.4	
	8	CE-I				MS	.439	.445		.282	17.1	123	.848	9120.7	70%
R18	9	CC	5	60	27	Norm	.484	.601		.159		136	.815	9498.4	
	10	CE-I				MS	.478	.551		.175	26.5	115	.852	9367.9	58%
	11	CC (75%)	5	60	27	Norm	.486	.454		.280		147	.728	9107.5	
	12	CE-I (75%)				MS	.523	.397		.344	23.5	112	.777	8920.9	53%

Note: RW17 = Rehder and Waldmann (2017); RB05 = Rehder and Burnett (2005); R15 = Rehder (2015); R18 = Rehder (2018). CC = common cause network; CE = common effect network. CE-I and CE-C denote common effect networks with independent and conjunctive causes, respectively. Norm = normative model. MS = mutation sampler. AIC = Akaike's information criterion.

9 | APPENDIX D: MODEL FITS TO CAUSAL CATEGORIZATION STUDIES

The normative model and the mutation sampler were fit to causal categorization data from 25 experimental conditions reported in seven articles. In every condition, subjects were first taught categories whose binary features were causally related. The example of Myastars presented in the main text was one member of a set of six experimental categories that included biological kinds (species of ants and shrimp), non-living natural kinds (types of stars and molecules), and artifacts (types of cars and computers). To ensure that subjects learned the category's features and causal relations they were required to pass an extensive multiple choice test. The items presented on the subsequent classification test consisted of a set of features (e.g., a star with ionized helium, normal temperature, a large number of planets, etc.).

Rehder and Hastie (2001, Experiment 2) (referred to as RH01 in Table 6) taught subjects categories with four binary features. In one condition the features formed a common cause network (one feature caused the other three). In another they formed a common effect network (one feature was caused by the other three). In all conditions subjects were told that one feature on each binary dimension occurred in 75% of category members and that the other occurred in 25% of category members (e.g., that 75% of Myastars have high density and 25% have normal density). Test items consisted of all 16 items that can be formed from four binary dimensions. For purposes of fitting, those 16 items were aggregated into 8 distinct types, formed by crossing the presence versus absence of X and the number of Y features present (0-3).

Rehder (2003a) (R03a) also taught subjects categories whose four features formed either a common cause or common effect network. Unlike Rehder and Hastie (2001), in this experiment subjects were not given the 75/25% feature base rate information. There were 16 test items of 8 distinct types. Rehder (2003b) (R03b) taught subjects categories whose four features formed a causal chain ($W \rightarrow X \rightarrow Y \rightarrow Z$). 75/25% feature base rate information was provided in Experiment 1 but not Experiment 2. There were 16 test items of 8 distinct types.

Rehder and Kim (2006) (RK06) taught subjects categories with five binary features. In Experiment 1, subjects performed two within-subject conditions that varied the causal knowledge that was provided. In one, the "212" condition, two features caused one feature, which in turn causes two features. In the other, three of the five features formed a causal chain (one of two sub-networks of the 212 network, counterbalanced over subjects, which ensured that comparisons between conditions involved the same category features. Experiment 2 consisted of a "311" condition (three features caused one feature, which caused another feature) and a causal chain (one of three sub-networks of the 311 structure). Experiment 3 consisted of a "113" condition (one feature causes one feature, which causes three features) and a causal chain (one of three sub-networks of the 113 structure). In all three experiments, one feature on each binary dimension was described as occurring in "most" category members while the other features was described as occurring in "some" category members. There were 32 test items, aggregated into various numbers of distinct types depending on the condition.

Rehder and Kim (2008) (RK08) taught subjects categories with four binary features that formed a causal chain. The unipolar condition was like the previous experiments in that the values on the binary dimensions were either "normal" or value that was distinct from normal (e.g., "Most Myastars have high density whereas some have normal density."). In contrast, in the bipolar condition there were two distinct (i.e., non-normal) values on each dimension (e.g., "Most Myastars have high density whereas some have low density."). There were 16 test items of 16 distinct types.

Rehder and Kim (2010) (RK10) taught subjects categories with three binary features that formed a causal chain ($X \rightarrow Y \rightarrow Z$). Experiment 1 included two conditions. In the strong condition, subjects were told that each cause feature brought about its effect 100% of the time. In the weak condition, they did so 75% of time. In the "weak-alt" condition of Experiment 2 subjects were told that each effect feature had no cause other than its parent in the causal

chain. In the “strong-alt” condition they were told that each effect feature would occur with probability 50% even when its parent cause in the causal chain was absent. Two additional experiments testing a three-element causal chain were reported in Appendix B of Rehder and Kim (2010). The first manipulated causal strength between 100% and 75% (as in Experiment 1) but subjects were additionally told that each effect had no other causes. The second manipulated causal strength between 90% and 60%. In all experiments, one feature on each binary dimension was described as occurring in “most” category members and the dimensions were bipolar (as in Rehder and Kim (2008), above). There were 8 test items, except for the final 90%/60% experiment in which there were 16 (each distinct test item was presented twice).

As described in Appendix C, Rehder (2015) (R15) taught subjects categories with six binary features. These features formed an independent and conjunctive common effect sub-network (Experiment 1), two independent common effect sub-networks (Experiment 2, independent condition), or two conjunctive common effect sub-networks (Experiment 2, conjunctive condition). Causal strength was manipulated within each condition of Experiment 2. Subjects rendered not only conditional probability judgments (as described in Appendix C) but also categorization judgments. In each experiment there were 16 test items of 12 distinct types.

The aggregate classification ratings in each condition were fit according to

$$\text{rating}(t_i) = 100 * p_{M,\theta_M}(t_i)^\gamma$$

where t_i is a test items, M is a model, and θ_M are its parameters. The normative model had the same causal model parameters as in Appendix C; the mutation sampler had an additional *bias* parameter (constrained to the range 0-1). Parameter γ (range 0-4) provides a nonlinear power transformation of a model's predicted joint probability¹⁹. The result was then multiplied by 100 to scale it onto the 0-100 rating scale. The model fitting procedure again minimized squared error. Table 6, which has the same format as Table 5 in Appendix C, presents the results of fitting the classification data. It shows that the mutation sampler yielded a better fit (correcting for the number of parameters) as compared to the normative model in 21 of the 25 experimental conditions.

¹⁹The power transformation allows the evidence for category membership provided by each feature in a test item to be integrated in a manner other than multiplication. Examination of Table C1 indicates that the fits yielded values of γ in the range [0.1, 0.4]. The transformation specified by a γ in this range is very similar to a logarithm. That is, subjects tended to add rather than multiply the evidence for category membership provided by each feature. See Griffiths and Tenenbaum (2005) and Rehder (2015) for examples of power function transformations.

TABLE 6 Fits of the normative model and the mutation sampler to past causal categorization studies. AIC values in bold italic red reflect cases in which the mutation sampler yielded a better fit as compared to the normative model.

Study	Expt.	Condition	No. of network variables	No. of subjects	No. of judgment types	Model	Parameters						Measures of fit		
							c	m	m_2	b	λ	bias	γ	R	AIC
RH01	2	CC	4	78	8	Norm	.940	.756	.444				.166	.988	25.4
		CE-I				MS	.978	.739	.587	43.7	.392		.168	.999	11.9
	2	CE-C				Norm	.821	.615	.317				.166	.998	12.3
						MS	.814	.602	.322	64.0	.985		.166	.998	16.3
R03a	CC		4	36	8	Norm	.895	.733	.294				.170	.981	28.1
		CE-I				MS	.933	.630	.410	10.5	.685		.174	1.000	-14.4
	CE-I					Norm	.700	.890	.003				.142	.965	37.1
						MS	.623	.833	.004	4.2	.902		.143	.997	21.4
R03b	1	Chain	4	36	16	Norm	.931	.613	.735				.164	.986	41.6
						MS	.941	.559	.775	64.0	.942		.159	.988	43.0
	2	Chain	4	36	16	Norm	.722	.867	.258				.255	.910	71.7
						MS	.546	.603	.284	3.4	.771		.241	.979	53.2
RK06	1	212	5	72	18	Norm	.889	.470	.800				.135	.993	33.2
						MS	.584	.308	.424	3.0	1.000		.129	.998	13.4
	Chain		3	72	8	Norm	.747	.346	.648				.304	.998	7.9
						MS	.772	.271	.698	64.0	.210		.304	1.000	-2.8
RK08	2	311	5	72	16	Norm	.862	.448	.830				.144	.987	42.9
						MS	.860	.395	.851	64.0	.995		.142	.988	45.8
	Chain		3	72	8	Norm	.718	.331	.602				.333	.982	22.4
						MS	.517	.078	.431	3.4	.935		.333	.991	20.8
RK10	3	113	5	72	16	Norm	.925	.473	.686				.171	.964	56.5
						MS	.793	.347	.370	3.8	.998		.152	.992	36.8
	Chain		3	72	8	Norm	.799	.522	.561				.318	.985	24.4
						MS	.627	.206	.449	3.4	.917		.316	1.000	4.5
RK08	Bipolar		4	36	16	Norm	.871	.920	.320				.269	.908	77.1
						MS	.549	.603	.226	2.7	.892		.256	.982	56.2
	Unipolar		4	36	16	Norm	.939	.545	.709				.180	.972	52.6
						MS	.839	.312	.500	3.7	.993		.172	.987	44.8
RK10	1	Chain (weak)	3	36	8	Norm	.866	.894	.307				.284	.950	40.0
						MS	.647	.555	.310	2.0	.882		.271	.997	22.1
	Chain (strong)		3	36	8	Norm	.855	.980	.122				.365	.975	38.5
						MS	.623	.816	.255	2.0	.859		.372	.994	30.6
RK10	2	Chain (weak alt.)	3	36	8	Norm	.834	.899	.187				.352	.974	35.7
						MS	.644	.617	.193	2.6	.841		.346	.996	25.4
	Chain (strong alt.)		3	36	8	Norm	.870	.848	.562				.248	.983	30.2
						MS	.587	.665	.332	2.7	.965		.228	1.000	-15.1
App	App	Chain (no alt., weak)	3	36	8	Norm	.915	.936	.156				.337	.979	35.9
						MS	.717	.719	.132	2.5	.919		.325	.995	28.2
	Chain (no alt., strong)		3	36	8	Norm	.802	.999	.005				.315	.989	35.3
						MS	.491	.970	.026	2.0	.782		.340	.993	35.3
App	App	Chain (60%)	3	48	8	Norm	.888	.891	.374				.290	.963	37.9
						MS	.688	.561	.362	2.0	.912		.276	.998	16.6
	Chain (90%)		3	48	8	Norm	.865	.758	.432				.316	.962	36.1
						MS	.594	.433	.234	2.7	.918		.307	.997	19.8
R15	1	CE-I & CE-C	6	48	12	Norm	.823	.855	.977	.278			.286	.981	47.7
						MS	.729	.862	.970	.150	29.1	1.000	.267	.992	41.0
	2	CE-I (weak) & CE-I (strong)	6	48	12	Norm	.871	.402	.733	.742			.246	.991	39.5
						MS	.861	.382	.721	.735	64.0	1.000	.245	.990	44.4
R15	CE-C (weak) & CE-C (strong)		6	48	12	Norm	.846	.847	.914	.600			.283	.991	36.7
						MS	.853	.819	.899	.632	47.1	.863	.281	.994	35.9

Note: RH01 = Rehder and Hastie (2001); R03a = Rehder (2003a); R03b = Rehder (2003b); RK06 = Rehder and Kim (2006); RK08 = Rehder and Kim (2008); RK10 = Rehder and Kim (2010); R15 = Rehder (2015). CC = common cause network; CE = common effect network. CE-I and CE-C denote common effect networks with independent and conjunctive causes, respectively. Norm = normative model. MS = mutation sampler. AIC = Akaike's information criterion.

10 | APPENDIX E: MODEL FITS TO INTERVENTION EXPERIMENTS

The models were fit to the four intervention experiments reported in Waldmann and Hagmayer (2005). Experiments 1 and 2 are described in the main text. In Experiments 3 and 4 all subjects were instructed on the common cause structure shown in Fig. 6J. In Experiment 3 the marginal probability, or “base rate” of the common cause (P in Fig. 6J) as it appeared in the training data was manipulated. In the high base rate condition P was present in 16 of the 20 training instances whereas in the low base rate condition it was present in only 4 instances. In Experiment 4 the strengths of the causal relations was manipulated such that one of the causal links in the common cause structure was strong while the other was weak (see Waldmann & Hagmayer, 2005, for details).

The aggregate ratings in each experiment were fit according to

$$\text{rating}(t_{ij}) = s * p_{M_i, \theta_{M_i}}(t_{ij})$$

where M_i is a model, θ_{M_i} are its parameters, and t_{ij} is a query about M_i . The model varied depending on experimental condition (between Model A and Model B in Experiment 1, between a Common Cause and Chain model in Experiment 2, etc.) and whether the antecedent given in the test item was described as resulting from an observation or an intervention. For example, when Model A subjects in Experiment 1 were asked to rate $p(S = 1|H = 1)$ (i.e., to predict the presence of S given that H was observed present) then Model A was used to generate the conditional probability of S given H . But when subjects were asked to rate $p(S = 1|do(H = 1))$ (i.e., to predict S when the presence of H was due to an intervention) then graph surgery was performed on Model A (i.e., the causal link between P and H) was removed before the conditional probability of S given H was computed. In Experiments 1 and 2 the causal models had the same parameters as in Appendix C (c , m , b , and s for the normative model; the additional parameters for the samplers were λ and *bias*). Because Experiment 3 manipulated the base rate of the common cause, the fits in that experiment included two c parameters (for the high and low base rate conditions, respectively). Because Experiment 4 manipulated the strengths of the causal relationships, the fits in that experiment included two m parameters.

Table 7 presents the results of fitting the intervention data. It shows that the mutation sampler yielded a better fit than the normative model in all four experiments in Waldmann and Hagmayer (2005).

Exp.	No. of network variables		No. of judge types		Model	Params						Measures		of fit
						<i>c</i>	<i>c</i> ₂	<i>m</i>	<i>m</i> ₂	<i>b</i>	λ	bias	R	AIC
1	5	50	8	Norm.	0.270		0.965			0.032			0.973	16.9
				MS	0.078		0.914			0.034	62.5	0.320	0.996	5.9
2	3	48	8	Norm.	0.393		0.795			0.084			0.990	4.1
				MS	0.388		0.749			0.109	18.5	0.101	>0.999	-24.1
3	3	32	8	Norm.	0.506	0.232	1.000			0.140			0.968	16.6
				MS	0.436	0.032	1.000			0.144	20.0	0.422	0.993	7.69
4	3	32	8	Norm.	0.530		1.000	0.567	0.076				0.974	8.99
				MS	0.837		0.966	0.398	0.063	40.0	0.001		0.996	-2.44

TABLE 7 Fits of normative model and mutation sampler to all experiments from Waldmann and Hagmayer (2005).

We note that the excellent quantitative fit of the mutation sampler in Fig. 6I may be due to the overfitting, a possibility that arises because of the relatively small number of conditional probability judgments that participants were asked in these experiments. For this reason, we believe that the more important theoretical point is that the mutation sampler can account qualitatively for a violation of independence in the context of interventions that the normative model cannot.

11 | APPENDIX F: SAMPLING FOR CONDITIONAL PROBABILITY QUERIES

Fig. 12 presents the rates of convergence for six conditional probability queries associated with the five-variable network presented earlier in Fig. 2 as a function of chain length (λ). Each panel shows the conditional probability computed by the normative model (red), the mutation sampler (black), and the alternative sampler in which states where the conditional probability query's antecedent are true are ten times more likely to be sampled than those in which it is false (blue). In each panel the alternative sampler converges faster than the standard one. Moreover, this effect is larger as the number of variables involved in the antecedent increases: The advantage for the alternative sampler is larger in the bottom row in Fig. 12, which presents conditional probability queries whose antecedents include four variables, than it is in the top row, which presents queries whose antecedents include only two variables. These results show that the mutation sampler can compute reasonably accurate conditional probability queries in a large network with even a modest number of samples.

Fig. 12 presents the rates of convergence for six conditional probability queries associated with the five-variable network presented earlier in Fig. 2 as a function of chain length (λ). Each panel shows the conditional probability computed by the normative model (red), the mutation sampler (black), and the alternative sampler in which states in which the conditional probability query's antecedent are true are ten times more likely to be sampled than those in which it is false (blue). In each panel the alternative sampler converges faster than the standard one. Moreover, this effect is larger as the number of variables involved in the antecedent increases: The advantage for the alternative sampler is larger in the bottom row in Fig. 12, which presents conditional probability queries whose antecedents include four variables, than it is in the top row, which presents queries whose antecedents include only two variables. These results show that the mutation sampler can compute reasonably accurate conditional probability queries in a large network with even a modest number of samples.

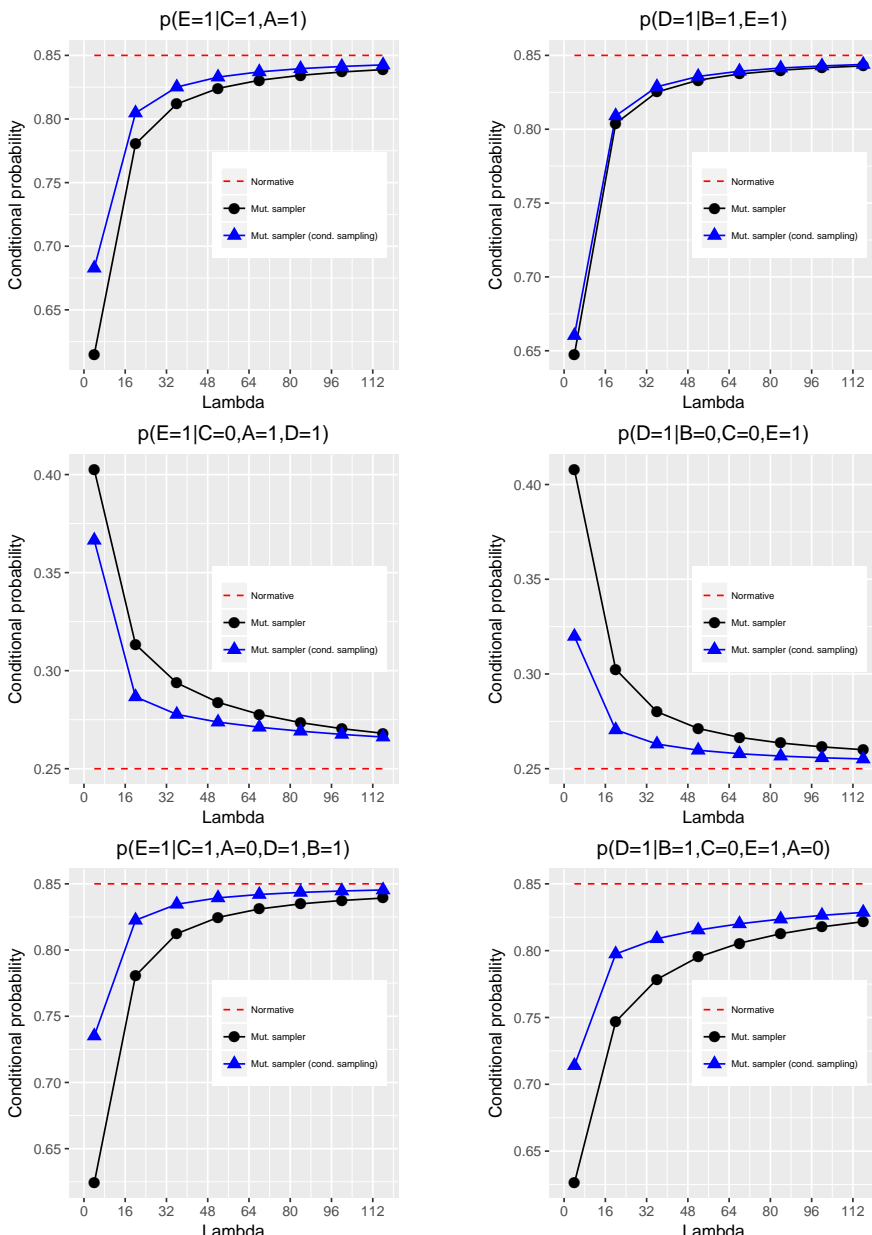


FIGURE 12 Six conditional probability judgments generated by the normative model (red), the standard mutation sampler (black), and the mutation sampler with an alternative proposal distribution (blue). Marginal probability of root causes = .50; causal strengths = .80, and strength of alternative causes = .25.

Model	Rehder (2018), Experiment 2, Common Cause Condition	Rehder & Kim (2010), Experiment 1, Weak Condition	Waldmann & Hagmayer (2005), Experiment 1	Causal Representations, Common Effect Condition
Normative	9495.4	40.0	16.9	993.2
Unbiased Egalitarian Sampler	9624.6	41.1	17.4	1115.5
Egalitarian Sampler	9249.4	34.5	5.9	795.4
Unbiased Sampler	9358.3	42.0	31.2	981.1
Mutation Sampler	9120.7	22.1	2.9	793.4

TABLE 8 AIC values of alternative models defined by dropping core principles of the mutation sampler for particular empirical data sets.

12 | SUPPLEMENTARY MATERIALS

Each of the sections below describe the results of fitting the four alternative sampling models to a particular empirical data set. Table 8 presents AICs for each of these data sets for each model. The fits of these models to any other data set reported in this article are available from the authors.

12.1 | Causal Reasoning

Table 2 in the main text indicates that the mutation sampler not only provided a better fit than the normative model but also each of the alternative sampling models in which one or more of the four principles were relaxed. To exemplify their differences, we now present the fits of each of these models to one particular data set, namely, the condition in Experiment 2 of Rehder (2018) that tested an extended common cause graph ($Z_A \leftarrow Y_A \leftarrow X \rightarrow Y_B \rightarrow Z_B$). The four panels in Fig. 13 present the fit of the unbiased egalitarian sampler (panel A), the unbiased sampler (panel B), the egalitarian sampler (C), and the mutation sampler (D), superimposed on the empirical data and the fit of the normative model. The x-axis in each panel present four pairs of conditional probability queries. Due to the Markov condition, each pair of conditional probabilities should be equal. For example, $p(z_i^1 | x^0 y_i^0 y_j^0 z_j^0)$ should equal $p(z_i^1 | x^0 y_i^0 y_j^0 z_j^1)$ even though Z_j is stipulated to equal 0 in the former versus 1 in the later. This is so because the value of Z_j is screened off from Z_i by the values of X , Y_i , and Y_j . The fits of the normative model in Fig. 13 indicate that each pair of adjacent conditional probability judgments should reflect independence.

Fig. 13 indicates that the unbiased egalitarian sampler is a poor account of these data as its fit does not differ appreciably from that of the normative model. The unbiased and egalitarian samplers account for some the independence violations, namely, that $p(z_i^1 | x^0 y_i^0 y_j^0 z_j^0) < p(z_i^1 | x^0 y_i^0 y_j^0 z_j^1)$ and $p(z_i^1 | x^1 y_i^1 y_j^1 z_j^0) < p(z_i^1 | x^1 y_i^1 y_j^1 z_j^1)$ (those pairs on the far left and far right of each panel in Fig. 13). However, they do not account for others, namely, $p(z_i^1 | x^0 y_i^0 y_j^1 z_j^0) < p(z_i^1 | x^0 y_i^0 y_j^1 z_j^1)$ and $p(z_i^1 | x^1 y_i^1 y_j^0 z_j^0) < p(z_i^1 | x^1 y_i^1 y_j^0 z_j^1)$ (the two interior pairs). In contrast, Fig. 13 reveals that the mutation sampler provides a full account of the observed pattern of independence violations in this experiment and Table 8 shows that it provides the best quantitative fit.

Why do the unbiased, egalitarian, and mutation samplers differ in the independence violations they account for? First, the egalitarian and mutation samplers differ in their preferences for coherence in network states (where coherence refers to the proportion of variables in a state that have the same value). The mutation sampler instantiates a

graded preference for coherence—the more variables with equal values, the better. This is so because, by making small adjustments to one of the (maximally coherent) prototype states, the mutation sampler also oversamples the mostly coherent neighboring states (those with 4 equal values) relative to other, less coherent states (those with 3 equal values). In contrast, because the egalitarian sampler can transition to any state, it does not oversample the mostly coherent states. As a result, although both models reproduce the independence violations in Fig. 13 when the conditional probability queries involve a comparison between graph states with 4 and 5 equal values, only the mutation sampler does so when they involve states with 3 and 4 equal values. These findings provide empirical evidence in favor of the mutation sampler’s proposal distribution. Second, the unbiased and mutation samplers differ in the means via which independence violations are produced. Whereas the mutation sampler’s independence violations depend primarily on its initial preference for prototype states, the unbiased sampler’s arise because the MH sampling dynamics are such that the relative probability of network states change as the length of the sampling chain increases. Independence violations that mirror the ones that subjects commit can arise for certain favorable causal model parameter values. As Fig. 13 indicates however, those favorable parameter values reproduce some but not all of the independence violations.

12.2 | Causal Categorization

Table 2 in the main text indicates that the mutation sampler also provided a better fit than the alternative samplers. Fig. 14 presents the fits of all four sampling models to the weak condition from Experiment 1 of Rehder and Kim (2010) that tested a chain graph ($X \rightarrow Y \rightarrow Z$). The four panels in Fig. 14 present the fit of the four samplers superimposed on the empirical data and the fit of the normative model. The x-axes present the categorization judgments that subjects were asked to make.

Fig. 14 indicates that both unbiased samplers provide a poor account of these data as their fits do not differ appreciably from the normative model’s. The egalitarian sampler fares better as it accounts for data points that the unbiased samplers do not (in particular, $p(x^0y^0z^1)$ and $p(x^0y^0z^1)$). Nonetheless, it incorrectly predicts the relative order of others ($p(x^1y^0z^1)$ and $p(x^1y^1z^0)$). Table 8 shows that the mutation sampler provides the best account of the data from this experiment.

12.3 | Causal Interventions

Table 2 in the main text shows that the mutation sampler provided a better fit than the alternative samplers and Fig. 15 presents the fits of all four sampling models to Experiment 1 of Waldmann and Hagmayer (2005). The figure indicates that the unbiased egalitarian sampler is a poor account of these data as its fit does not differ appreciably from that of the normative model. The other three models perform better as they are able to reproduce the key difference between $p(s^1|do(h^1))$ and $p(s^1|do(h^0))$. Nevertheless, Table 8 shows that the mutation sampler yielded the best quantitative fit.

12.4 | Causal Representations

Fig. 15 presents the fits of the four sampling models to the common effect coins experiment. It indicates that the fits of both unbiased samplers do not differ appreciably from the normative model’s. Although Table 8 indicates that the fit of the mutation sampler was slightly better than that of the egalitarian sampler, Fig. 15 shows that the fits of these two models were qualitatively identical.

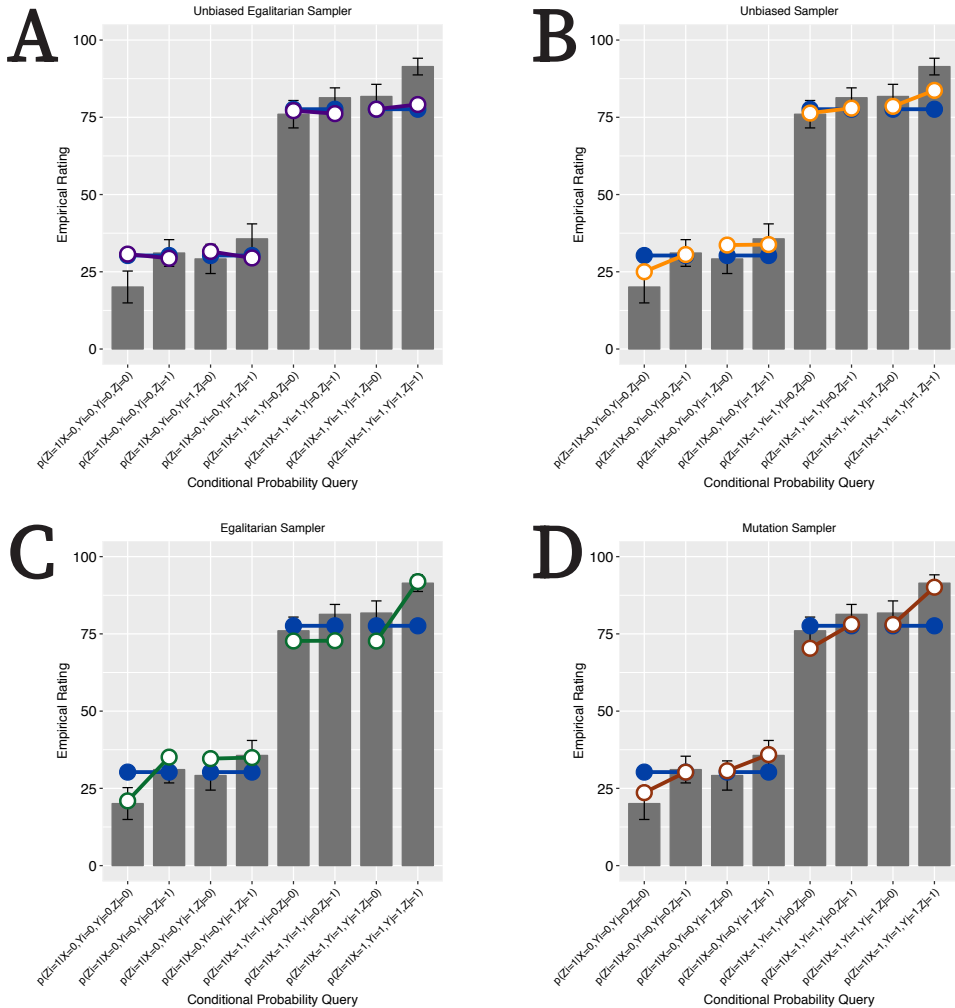


FIGURE 13 Fits of alternative models to Experiment 2 of Rehder (2018).

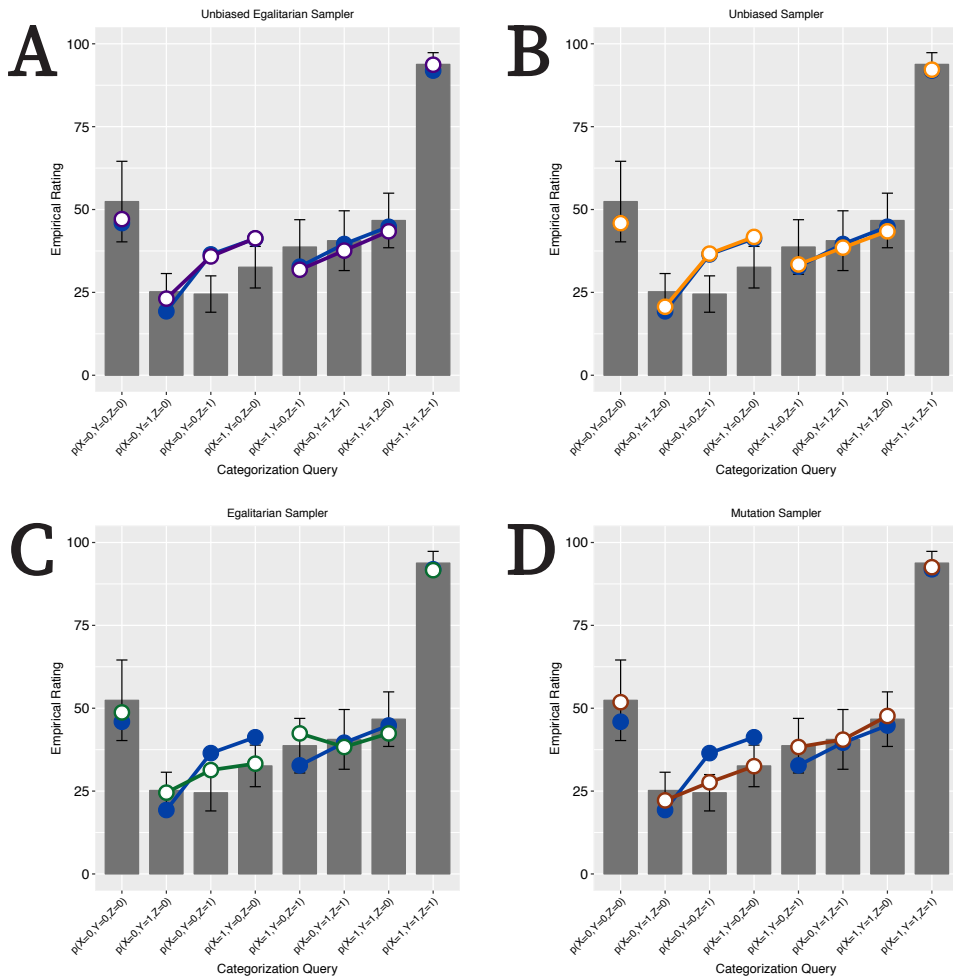


FIGURE 14 Fits of alternative models to Experiment 1 of Rehder and Kim (2010).

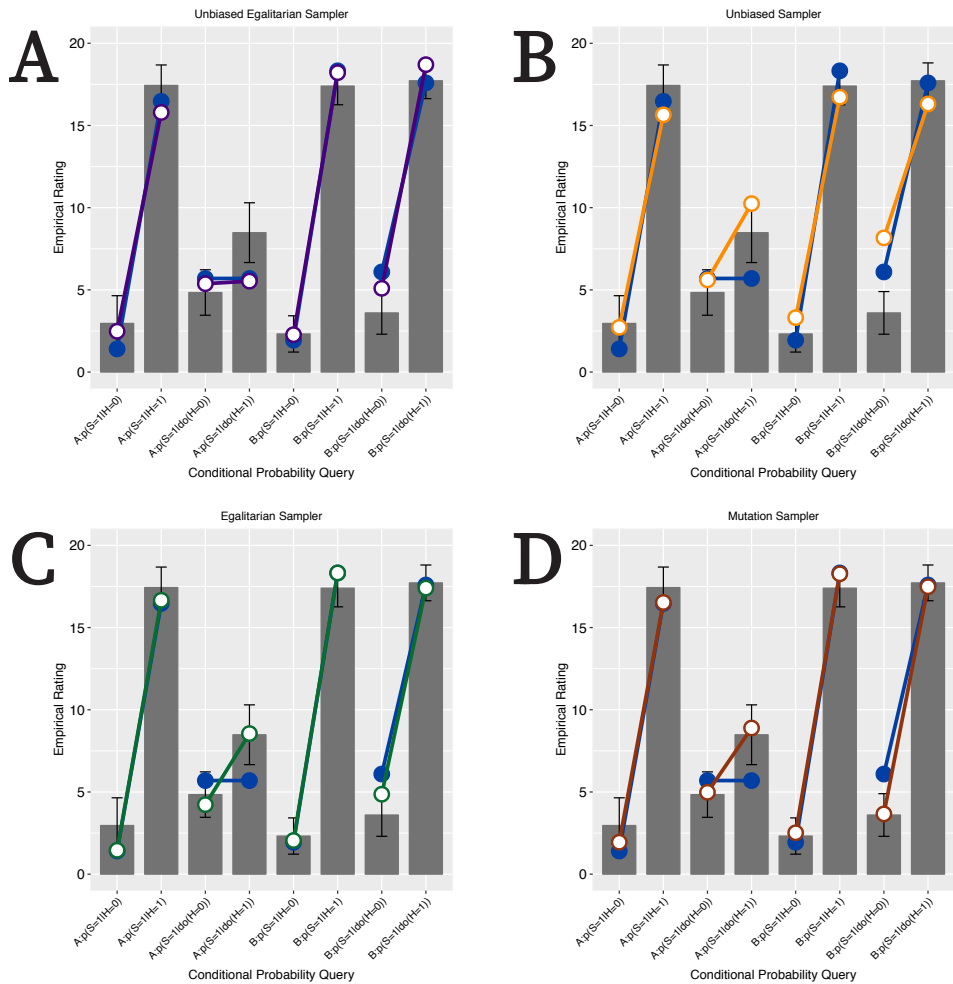


FIGURE 15 Fits of alternative models to Experiment 1 of Waldmann and Hagtmaier (2005).

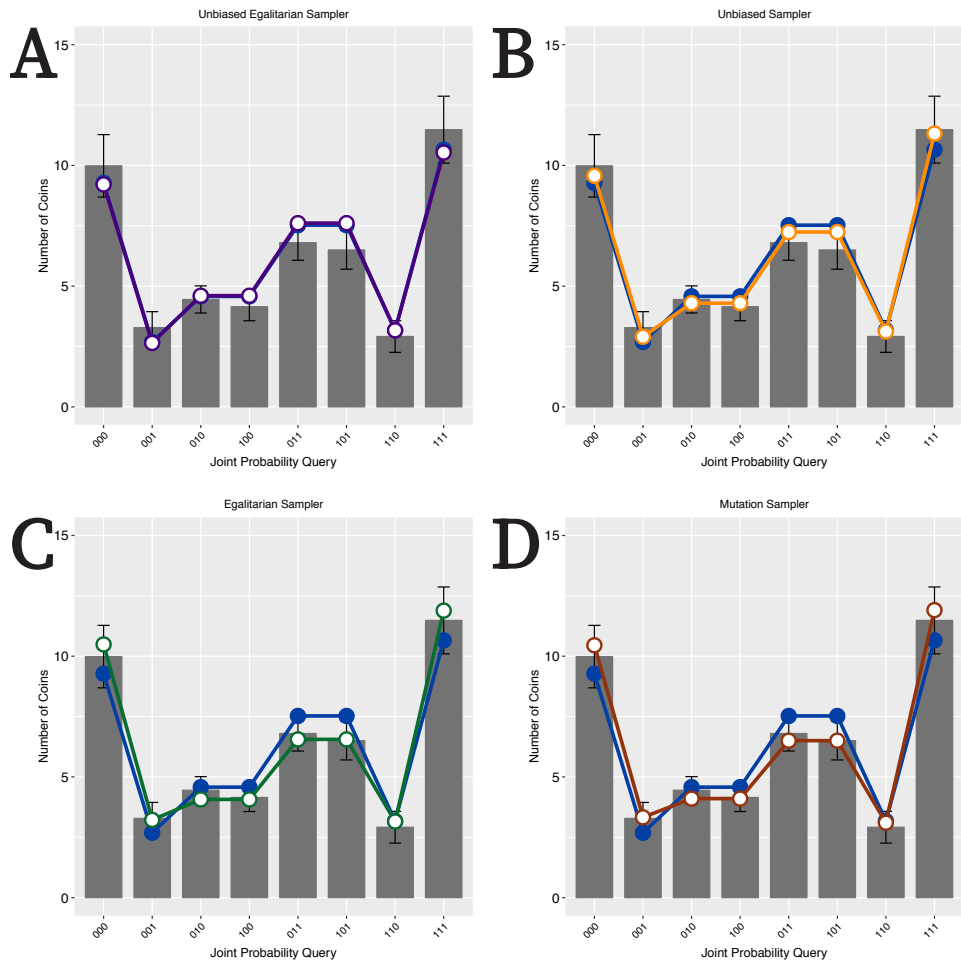


FIGURE 16 Fits of alternative models to the common effect coins experiment.